ABSTRACT

Title of Thesis: APPLICATION OF DIAGNOSTICS AND PROGNOSTICS TECHNIQUES TO QUALIFICATION AGAINST WEAR-OUT FAILURE

Abhishek Ram, Master of Science, 2022

Thesis Directed By: Dr. Diganta Das,

Department of Mechanical Engineering

Qualification is a process that demonstrates whether a product meets or exceeds specified requirements. Testing and data analysis performed within a qualification procedure should verify that products satisfy those requirements, including reliability requirements. Most of the electronics industry qualifies products using procedures dictated within qualification standards. A review of common qualification standards reveals that those standards do not consider customer requirements or the product physics-of-failure in that intended application. As a result, qualification, as represented in the reviewed qualification standards, would not meet our definition of qualification for reliability assessment.

This thesis provides an application-specific approach for developing a qualification procedure that accounts for customer requirements, product physics-of-failure, and knowledge of product behavior under loading. This thesis provides a revamped approach for developing a life cycle profile that accounts for loading throughout manufacturing/assembly, storage and transportation, and operation. The thesis also discusses identifying variations in the life cycle profile that may arise throughout the product lifetime and methods for estimating loads. This updated approach for developing a life cycle profile supports better failure prioritization, test selection, and test condition and duration requirement estimation.

Additionally, this thesis introduces the application of diagnostics and prognostics techniques to analyze real-time data trends while conducting qualification tests. Diagnostics techniques identify anomalous behavior exhibited by the product, and prognostics techniques forecast how the product will behave during the remainder of the qualification test and how the product would have behaved if the test continued. As a result, combining diagnostics and prognostics techniques can enable the prediction of the remaining time-to-failure for the product undergoing qualification. Several ancillary benefits related to an improved testing strategy, parts selection and management, and support of a prognostics and health management system in operation also arise from applying prognostics and diagnostics techniques to qualification.

APPLICATION OF DIAGNOSTICS AND PROGNOSTICS TECHNIQUES TO

QUALIFICATION AGAINST WEAR-OUT FAILURE

By

Abhishek Ram

Thesis submitted to the Faculty of the Graduate School of the
University of Maryland, College Park, in partial fulfillment
of the requirements for the degree of
Master's of Science
2022

Advisory Committee:

Dr. Diganta Das, Chair

Professor Abhijit Dasgupta

Professor Peter Sandborn

Dr. Michael Azarian

Acknowledgments

There are several different groups of people who helped me in developing and formulating this thesis. In no particular order, I will thank them accordingly. First, I would like to thank my advisor, Dr. Diganta Das, for his stalwart support throughout my time at the Center for Advanced Life Cycle Engineering and the University of Maryland. He brought me in during the peak of the COVID-19 pandemic and supported my personal growth goals while steering me in the right direction to ensure I could complete my thesis.

Secondly, I would like to thank the members of my committee (Professor Abhijit Dasgupta, Professor Peter Sandborn, and Dr. Michael Azarian) for their time as I defended my thesis and for providing feedback as necessary. Thirdly, I would like to thank the faculty in my research group (Professor Michael Pecht, Dr. Michael Osterman, Dr. Michael Azarian, and Dr. Robert Utter) for their support through daily morning meetings, where I had the opportunity to present several dozen times throughout my degree. Without their feedback and guidance, I know my thesis efforts and skills as a reliability engineer would not have reached the point that it has. I would also like to thank Dr. Robert Utter for his patience and time in onboarding me to use different laboratory equipment and for teaching me a lot about the failure analysis of different electronic products.

Additionally, I would like to thank the companies that support the Center for Advanced Life Cycle Engineering as part of the consortium. In particular, I would like to thank the companies (and the individuals I worked with in those companies) for their patience and their affability throughout the projects. Though I will not reveal their names, I hold them in the highest of regards. Another round of thanks goes to the Center for Advances in Reliability Safety (CAiRS) for allowing me to present twice and have very enlightening discussions on the future of reliability and safety.

I would also like to take this opportunity to thank my colleagues at the University of Maryland and particularly in CALCE. They provided me guidance/advice on navigating graduate school and life and ensured that even during my most stressed moments, I had something to laugh about. I have also had the opportunity to work with these folks on a variety of projects as well. Though there are countless others, a few people of the many people to whom I am hugely grateful are Lokesh Sangepu, Chintankumar Patel, Lekhith Yelamanchili, Ibaad Gandikota, Swarup Subudhi, Michel Raad, and Marco Jünger.

Last but certainly not least, I would like to thank my family: my mother, Nalini Vuppalapati, my father, Balakrishna Ram, and my brother, Aditya Sai Ram. Thank you to you all for the last 25 years of unconditional love.

Contents

List of Figures

List of Tables

1 Introduction to Qualification and the Updated Methodology

Edward Aloysius Murphy, Jr., a late aerospace engineer who worked on safety-critical systems, is best known for coining Murphy's Law: "anything that can go wrong will go wrong." Though Murphy touted this philosophy in the context of safety-critical systems, it still applies to product development and operation. An essential aspect of product development is validating that new products will successfully function and satisfy all operational requirements over their lifetime.

Product reliability demonstration in this thesis establishes that products can meet performance requirements in the intended application over the desired lifetime [1]. IEEE (Institute of Electrical and Electronics Engineers) 1624 [2]: "IEEE Standard for Organizational Reliability Capability" introduces reliability programs as the collection of practices that one can conduct for product reliability demonstration. IEEE 1624 lists eight examples of practices applicable for product reliability demonstration: (1) reliability requirements and planning; (2) training and development; (3) reliability analysis; (4) reliability testing; (5) supply chain management; (6) failure data tracking and analysis; (7) verification and validation; and (8) reliability improvements. Table 1 lists each of these reliability practices and the purposes of each practice.

Table 1: Key reliability practices in IEEE 1624 [2] and the purposes of each reliability practice.

Key Practices Defined in IEEE 1624	Purpose(s) of Each Key Practice
Reliability requirements and planning	Understand customer reliability requirements, generate product reliability requirements, plan the required reliability activities
Training and development	Enhance people's technical, business, and specialized strategic skills to design, assess, and manufacture reliable products effectively
Reliability analysis	Assess a product design or field performance to identify failure modes, mechanisms, and effects and to make reliability predictions
Reliability testing	Identify design weaknesses, explore design limits and environments, and demonstrate product reliability by running tests
Supply chain management	Proactively identify sources of items for satisfying product reliability requirements, create a list of items and suppliers for long-term business associations, manage suppliers on the contract
Failure data tracking and analysis	Collect manufacturing, functional testing, reliability testing, and field failure data for physical failure analysis, root cause analysis, statistical analysis of failure data, generate failure analysis reports
Verification and validation	Verify that planned reliability activities are implemented, validate outcomes of activities are consistent with results from other activities, validate that the product meets specified reliability requirements
Reliability improvements	Identification and implementation of product changes based on testing results, reported field failures, technological improvements, changing operating conditions, and other considerations

One reliability program activity used for assessing product reliability is qualification, which is a process that demonstrates if a product would meet or exceed some specified requirements. Qualification encompasses four key reliability activities: reliability requirements and planning, reliability analysis, reliability testing, and verification and validation. The purpose of reliability testing conducted during qualification is to demonstrate that products will satisfy those reliability requirements. Knowledge of failure modes, mechanisms, and effects identified from reliability analysis determines the tests to conduct for qualification. The qualification test conditions and durations should also stem from product reliability requirements.

IEEE 1332 [3] states that the reliability requirements for a reliability program should address (at minimum) the product functionality, duration, life cycle conditions, and reliability metrics for the product. Addressing product functionality includes measuring performance characteristics and demonstrating that the product operates within acceptable parameters. The duration is the desired/expected lifetime or mission time for the product in the intended application. Addressing life cycle conditions includes accounting for the effects of various loads the product experiences over its lifetime (e.g., during transport, storage, testing, handling, maintenance, operation, and variations therein). Reliability metrics are objective measures of performance and product durability over the product's life. When creating a qualification procedure for product reliability assessment, one should consider all these requirements.

1.1 Analyzing Qualification Standards' Capabilities for Reliability Assessment

Qualification is a product reliability assessment practice conducted by entities throughout the electronics industry. There are several standards dedicated to product qualification for various electronic products, and Table 2 includes some examples of these qualification standards. However, the question arises if the qualification procedure presented in qualification standards would satisfy the requirements of IEEE 1332 for developing a reliability program.

Table 2: Examples of qualification standards for some electronic products.

Electronic Product	**Qualification Standard Numbers**	**Qualification Standard Title**
Integrated Circuits	AEC-Q100 (Automotive Electronics Council)	Failure Mechanism Based Stress Test Qualification for Integrated Circuits [4]
	JESD47	Stress-Test-Driven Qualification of Integrated Circuits [5]
Discrete Semiconductors	AEC-Q101	Failure Mechanism Based Stress Test Qualification for Discrete Semiconductors in Automotive Applications [6]
	JEP148B (JEDEC Publication)	Reliability Qualification of Semiconductor Devices Based on Physics of Failure Risk and Opportunity Assessment [7]
Optoelectronic Semiconductors	AEC-Q102	Failure Mechanism Based Stress Test Qualification for Optoelectronic Semiconductors in Automotive Applications [8]

As part of an International Electronics Manufacturing Initiative (iNEMI) effort to develop an updated qualification procedure for new technologies and materials, Grosskopf et al. [9] reviewed the industry qualification and test method standards/publications listed in Table 3. The authors concluded that none of the standards included best practices for accounting for customer requirements and product physics-of-failure. An additional study of the other qualification standards in Table 2 by the author also revealed that these shortcomings are also present in those standards.

Recall that qualification as a reliability program activity relies on knowledge of product physics-of-failure within the intended product application to determine the qualification tests to conduct. Additionally, recall that each qualification test's test conditions and durations stem from knowledge of customer requirements and the intended application. Without providing strategies for determining customer requirements and accounting for product physics-of-failure, qualification conducted through these qualification standards would not meet the requirements set forth by IEEE 1332 for reliability programs.

Table 3: Industry qualification standards reviewed by Grosskopf et al. as part of iNEMI.

Standard Number	**Standard Title**
JESD47	Stress-Test-Driven Qualification of Integrated Circuits [5]
JESD94	Application-Specific Qualification Using Knowledge-Based Test Methodology [10]
JEP150	Stress-Driven Qualification of & Failure Mechanisms Associated with Assembled Solid-State Surface-Mount Components [11]
AEC Q100	Stress Test Qualification for Integrated Circuits [4]
MIL-STD 883 (U.S. Military Standard)	Test Method Standard for Microcircuits [12]
MIL-STD 750	Test Methods for Semiconductor Devices [13]

Grosskopf et al. [9] also surveyed 62 organizations between March and June 2018 regarding the package qualification methods, tools, and practices those organizations used. The organizations surveyed included original equipment manufacturers (OEMs), Electronics Manufacturing Services (EMSs), Integrated Circuit Package Assembly Houses (IC Houses), and others (e.g., wafer fabrication foundries, package material manufacturers, and universities). The breakdown of survey respondents is in Figure 1. The survey results revealed that approximately 70% of the respondents referenced qualification standards and used the test conditions and durations listed within the standards. 36% of those respondents who reference qualification standards also report that their intended application requirements exceed the test conditions and durations from the standard. Lastly, 61% of the respondents who reference qualification standards also saw the need for better aligning qualification practices with intended application requirements.

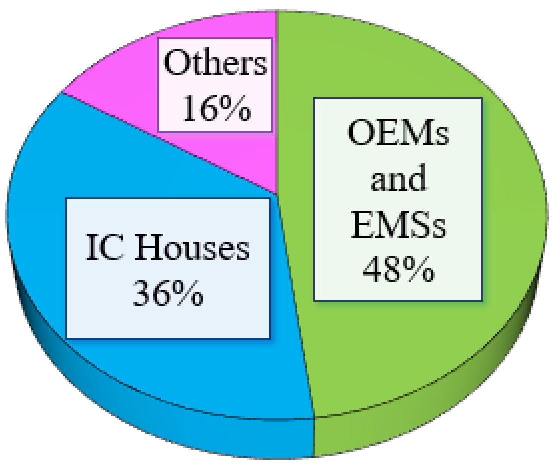

Figure 1: Breakdown of respondents to survey regarding qualification practices by Grosskopf et al. [9].

In their project summary report, Grosskopf et al. [14] provided examples of life cycle phases and loads experienced within those phases. However, the authors do not provide strategies for cataloging loads experienced by any products in their lifetime.

1.2 Proposed Application-Specific Qualification Procedure

Based on the literature review and study of qualification standards, there is a need for an updated industry guideline of best practices for product qualification. Existing qualification standards do not account for customer requirements and do not meet the reliability requirements stated by IEEE 1332 for complete reliability assessment. Qualification standards also do not leverage knowledge of the product physics-of-failure or measurable behavior under load conditions to develop efficient and effective qualification procedures. Many electronic product manufacturers or other component users continue to rely on qualifications conducted by the component manufacturer or recommended by qualification standards, assuming that the reported qualification meets the application requirements.

Additionally, component qualification as conducted by the electronic product manufacturer is often an unrealized opportunity to study the behavior of the component and electronic product before being placed into the intended application. Being able to study and document component behavior before operation can contribute to an improved, further-targeted qualification procedure, to component selection efforts, and to supporting condition monitoring and prognostics and health management systems in operation

The procedure presented in Figure 2 is an application-specific qualification procedure that (1) addresses the shortcomings of qualification procedures for product reliability assessment while also (2) taking advantage of additional benefits to studying product behavior. This thesis studies the development of a qualification procedure by an electronic product manufacturer conducting the qualification of a component or subsystem within the product to assess if the component or subsystem would meet the intended application requirements.

The subsequent chapters highlight each step in the proposed application-specific qualification procedure in greater detail. To summarize the procedure, in the first section, the qualification procedure relates to evaluating the life cycle profile, which allows accounting for the effects of loads experienced by the product over its lifetime. Next, conducting failure modes, mechanisms, and effects analysis identifies the different failure mechanisms that could impact the product lifetime, how those failure mechanisms would be detected/observed (failure modes), and the effects that the failure mechanisms would have on product behavior and eventual product failure. The combination of the life cycle loads from the life cycle profile and knowledge of product physics-of-failure leads to prioritizing the risk associated with failure due to different failure mechanisms. Failure mechanism risk stems from the likelihood of failure occurring due to a given failure mechanism and the severity of failure due to that risk.

The approach and focus of this thesis is qualification, where failure is expected to occur due to wearout failure mechanisms. Qualification for the purpose of evaluating the effects of overstress mechanisms is beyond the scope of this thesis. The approach is tailored to studying a single electronic component within an electronic product and cannot be immediately applicable to the qualification of systems without making modifications. The underlying assumption when conducting qualification is that one would need to run the test completely for the component to be qualified. This thesis does not study approaches to reducing the time and resources needed for application-specific qualification. The definition of failure during testing/qualification in this thesis is parametrically driven as the behavior under loading is monitored parametrically.

With the most critical failure mechanisms identified, one can decide on the required qualification tests to conduct. Using the life cycle profile results, the critical failure mechanisms, and corresponding acceleration factor models, one can determine the qualification condition and duration requirements for meeting the intended application requirements. Next, potential precursor parameters are identified using the critical failure mechanisms and via a study of historical testing data of similar products. The definition of product similarity is in Section 3.4. With knowledge of the precursor parameters to track, the next step is to assess different diagnostics and prognostics techniques using historical data and data from conducting component qualification. Some samples will be qualified for training, testing, and validation, respectively. With a finalized qualification procedure, one can identify and implement diagnostics and prognostics techniques to better analyze product behavior under load applications before introducing the product to the intended application and make qualification more targeted to the application requirements. Note that the validation of diagnostics and prognostics techniques actually involves a two-way relationship with identification of those techniques because the results of validation can impacts the identification results. This thesis does not discuss techniques for validating diagnostics and prognostics techniques (e.g., cross-validation.)

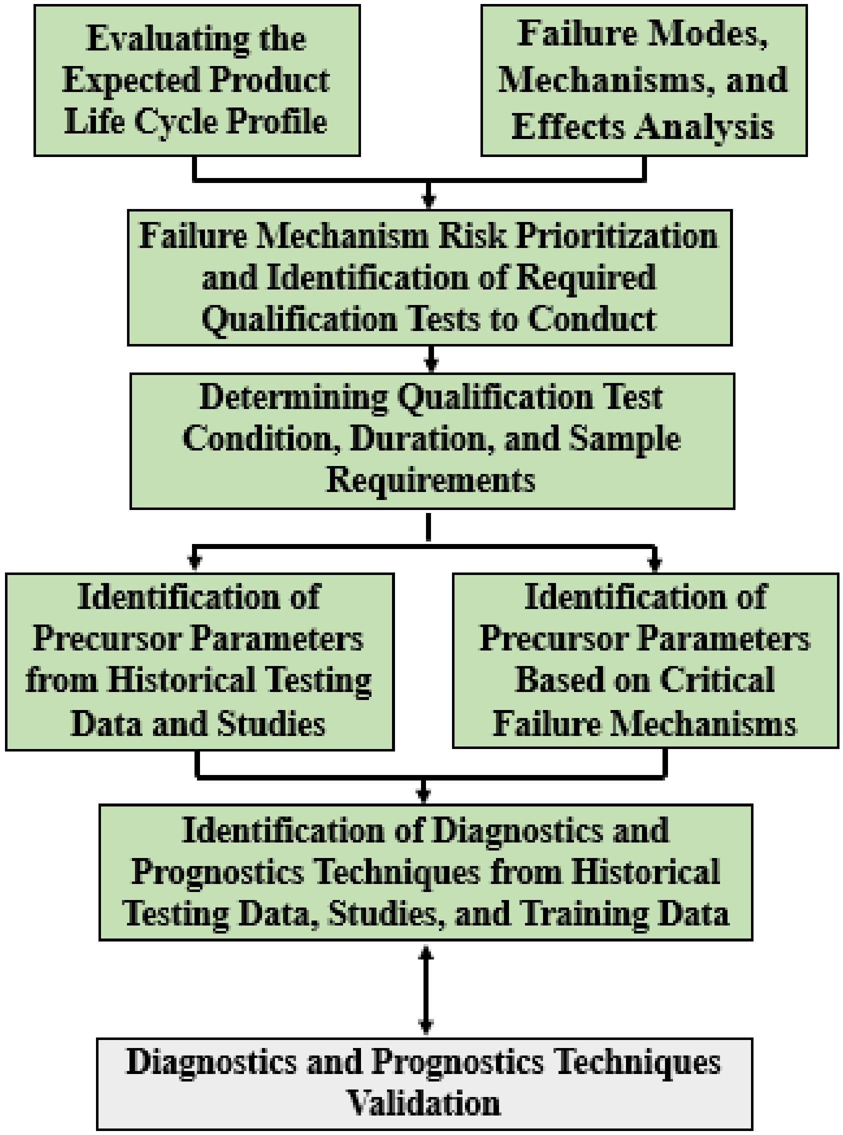

Figure 2: Application-specific qualification procedure for any electronic product for any intended application.

2 Evaluating the Product Life Cycle

The life cycle profile lists all the expected loads a product experiences across its lifetime. United States Military Standard 810 [15] separates the profile of the expected loads into the life cycle environmental profile and the life cycle profile. The life cycle environmental profile accounts for the environmentally-driven loads the product undergoes. In contrast, the life cycle profile includes stresses incurred due to exposure to nonenvironmental loads. In the product lifetime, there will be instances where the stresses incurred are driven predominantly by the environment (e.g., diurnal temperature cycling and humidity). Additionally, there will be instances where the stresses incurred are driven by nonenvironmental sources (e.g., packaging and handling, product assembly into a final product). There will also be instances where environmental and nonenvironmental loading sources simultaneously affect the product (e.g., diurnal temperature cycling during operation).

The life cycle profile development procedure outlined in this paper integrates the Military Standard 810-defined life cycle environmental profile and life cycle profile into a single profile, which includes all the expected loads a product will undergo across its lifetime, from the completion of product manufacture to the end of operation and removal from service [16]. The life cycle profile includes information on each requirement for product reliability demonstration, and subsequent discussion analyzes the purpose of the product life cycle profile in completing multiple reliability practices.

2.1 Review of Previous Life Cycle Studies

Several authors developed procedures or examples of life cycle profiles for different products and applications. For example, Ramakrishnan and Pecht [17] evaluated the loading experienced by a product during air and ground transportation. The authors shipped a computer monitor from College Park, Maryland, to San Pedro, California and back and measured the vibrations, temperatures, and humidity the product experienced during shipping and handling. Another example of a life cycle profile study is Valentin et al. [18] generated a life cycle profile for an advanced amphibious assault vehicle to complete virtual qualification. The authors accounted for the effects of temperature cycling, random vibration, and shock based on the information provided by United States Marine Corps personnel.

In a separate study, Valentin et al. [18] examined identified and recorded operational profiles for a preliminary electronic module design intended to support aircraft engines. The authors identified operational loads in the study as temperature cycle limits, average temperature, temperature cycling frequency, mechanical vibration, and electrical loads. The authors also highlighted that one can examine loads incurred during assembly, transportation, storage, handling, and rework and that one can obtain knowledge of life cycle loads using interviews with the manufacturer and end-user, measured data from the intended operational environment, and prior experience of similar products and applications.

Peyghami et al. [19] studied system-level reliability analysis for DC microgrids and noted that the microgrid system could experience several loads, including solar irradiance, wind speeds, temperature conditions, humidity, and the desired electrical load profile. The authors also noted that the environmental loads and electrical load profile depend on the geographical location, season, and energy resource management to support the microgrid power receivers. The authors also highlighted instances where some subsystems are idle, and other systems would need to operate to maintain power inputs to the microgrid power receivers, demonstrating variations in the operating profile for the whole system.

Ma et al. [20] researched the emulation and testing of power electronics within electric machine drive systems for various mission profiles. These mission profiles could include electric vehicles, aerospace, and high-speed rails. As part of this endeavor, the authors noted the mechanical loads, control strategies, transient loads, electromagnetic properties, abnormal conditions, and environmental conditions that can vary between different product mission profiles. The authors noted the mechanical loads induced by mechanical inertia preventing rapid changes in rotational speed and vibrations. The loads caused by the control strategies pertained to voltage and current load requirements changing with respect to torque requirements. Transient loads are high-frequency oscillations due to sudden changes in mission profile requirements. Air-gap magnetic field distortion, uneven distribution of magnetic resistance, and other non-ideal characteristics of the electric machine contribute to wave harmonic excitation, leading to torque ripples, flux distortion, and other distortions. Examples of abnormal conditions can include irregular voltages and currents leading to transients and high-amplitude harmonics. The authors cited that temperature and humidity are the environmental conditions that mainly effect reliability.

In their doctoral dissertation, Karppinen [21] explored the impacts of electrical, thermal, and mechanical loads on electronic assemblies during operation. Karppinen also mentioned chemical loads impacting product reliability, but it was beyond the scope of their discussion. Examples of external loads the author cited were electrostatic discharges, ambient temperature change, and drop impacts. Internal loads the author cited were high current densities and electric power dissipation. The author also provided examples of mechanical loads: shock impact, vibration, and static/quasi-static bending.

Cluff et al. [22] developed a general approach for characterizing airplane environments, particularly time-dependent thermal environments. The authors described that some factors that impact the board's thermal history include local self-heating, forced air cooling, global air temperature, flight speeds, altitude, solar radiation, and thermal mass effects of the airplane. The approach detailed by the authors included instrumentation to measure different operational parameters and facets of the environment, categorizing and cumulating cycles in terms of some key parameters, and determining box and board power cycle profiles to develop a complete operational life cycle profile.

The FIDES guide [23] lists several variations of operational life cycle profiles for multiple military and industrial applications. FIDES also guides how to form a life cycle profile from a qualitative perspective, especially accounting for the phases of the product lifetime, the location for each phase, the geographic or climatic region, and the type of use. FIDES also provides recommendations for quantitative approaches for calculating the loads experienced due to thermoelectric loads, temperature cycling, relative humidity, and vibration. The guide also provides qualitative approaches for considering the effects of chemical loads.

Military Standard 810 [15] states that the life cycle profile should describe the anticipated logistical and operational events the product experiences from the point of factory acceptance (described as the end of manufacture in this paper) to the end of the product's useful life. The life cycle profile should catalog the natural and induced environments (or combinations thereof) for each of these logistical and operational events. For each of these environments, the life cycle profile should include narrative, tabular, graphic, and statistical characterizations of the loads experienced by the product over its lifetime.

Military Standard 810 [15] also contends that developing the life cycle profile should be a shared effort between the product manufacturer and the customer. The product life cycle profile can account for loads incurred by the product during different logistical events (e.g., assembly, shipping/handling, transportation, rework, and storage) and operational events (e.g., normal operation, idle, repair/maintenance) using input from both product manufacturers and customers. With a collaboration between both parties, the life cycle profile can also successfully account for different environments for each event, durations of exposure to different loads across the life cycle, frequency of different life cycle phases, and other considerations.

Each of the previous life cycle profile studies/guides by Ramakrishnan and Pecht [17], Valentin et al. [24, 18], Peyghami et al. [19], Ma et al. [20], Karppinen [21], Cluff et al. [22], the FIDES guide [23], and Military Standard 810 [15] focused on different parts of the product life cycle and examined only some of the loads that the product could experience. Note that only the FIDES guide considered chemical loads and only provided qualitative approaches for characterizing those loads. Additionally, only Cluff et al. and the FIDES guide provided generalizable approaches for accounting for different loads, but both these approaches only studied product operation. Valentin et al. [18] highlighted that one could study the loads experienced by the product during assembly, transportation, storage, handling, and rework, but they did not provide strategies for identifying each intermediate source of loading within each of those life cycle phases. Without identifying individual procedures, one cannot thoroughly examine the loads the product would experience. Ramakrishnan and Pecht studied loads experienced by the product during air and ground transportation, but product transportation can also occur through the use of the sea, air, ground, or combinations therein. The FIDES guide, Peyghami et al., and Ma et al. were the only studies/guides that discussed and gave examples of variations that could occur in given operational applications. Finally, though Military Standard 810 guided on developing a life cycle profile, what to account for, and where to look for data, it does not provide direct guidance on characterizing different types of life cycle loads nor visual representations of the guidance it provides to demonstrate its recommendations.

The life cycle profile development procedure explained in this paper is highly inspired by the recommendations set forth by Military Standard 810 [15]. The test condition categorizations provided by Military Standard 810 also inspired the sample qualitative categorizations of life cycle loads described in the life cycle profile development procedure. The generalized approaches for identifying and characterizing loads described by Cluff et al. [22] and the FIDES guide [23] influence this paper's life cycle profile development procedure. However, this procedure also provides recommendations for accounting for a variety of loads beyond that which was discussed by Ramakrishnan and Pecht [17], Valentin et al. [24, 18], Cluff et al., and the FIDES guide. This procedure also examines possible variations in the product life cycle both before and during product operation, whereas the FIDES guide, Peyghami et al. [19], and Ma et al. [20] only looked at variations during operation. This procedure also provides more guidance on identifying life cycle phases and introduces the notion of life cycle steps to provide a more in-depth look at loads in each phase.

2.2 Using the Life Cycle Profile for Product Reliability Assessment

Developing a product life cycle profile completes part of the IEEE 1624-defined reliability practice of "reliability requirements and planning," as the life cycle profile accounts for the product reliability requirements in the intended application. Using the life cycle profile, the entity conducting qualification identifies reliability requirements for the product and can plan the appropriate reliability practices to demonstrate that product reliability requirements are met [2].

Figure 3 illustrates the process for developing the life cycle profile. The following sections describe the process for life cycle profile development.

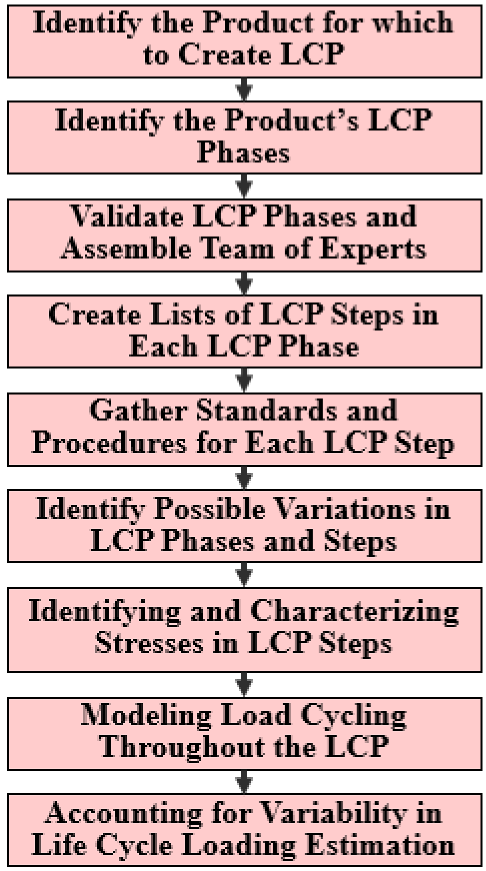

Figure 3: The procedure for developing a product life cycle profile (LCP).

The life cycle profile development procedure applies to any product. The procedure focuses on identifying as many loads as possible, including when loading histories are unavailable. The value of a comprehensive approach can lead to a better understanding of product loads and their effects on product reliability.

2.2.1 Determine the Product's Life Cycle Profile Phases

The product life cycle profile stretches across multiple phases of the product lifetime. These phases of the product lifetime are called life cycle profile phases. Examples of life cycle phases could include a certain period of operation, a particular manufacturing procedure, a combined storage and transportation step, or a maintenance and repair procedure. Figure 4 demonstrates examples of life cycle phases in a product life cycle that occur worldwide.

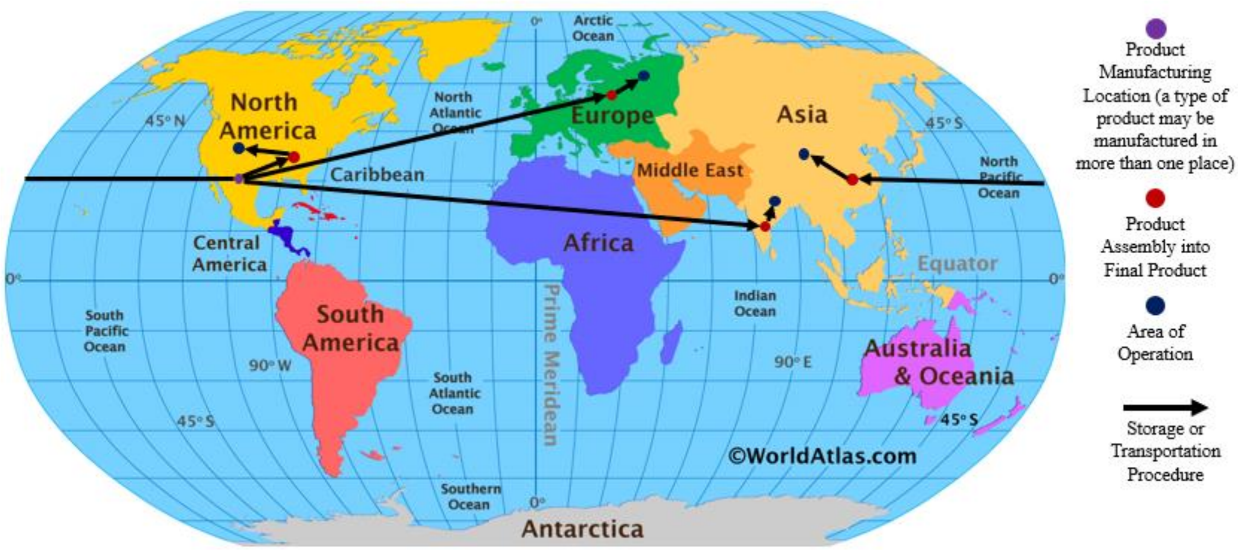

Figure 4: Examples of life cycle profile phases in a life cycle profile mapped worldwide. Note that the phases in these examples consist of product manufacturing, assembly into the final product, different storage/transportation procedures, and operation.

The FIDES guide [23] provides several examples for developing life cycle profiles and identifying phases within the life cycle profile. For instance, FIDES includes a workflow for identifying the life cycle profile of equipment mounted on a civil aircraft in the avionics bay for both medium-haul aircraft and aircraft with turboprop engines. FIDES also provides life cycle profile workflows for industrial system equipment, washing machines, and external stores in multi-role fighter aircraft.

2.2.2 Validate Life Cycle Profile Phases and Identify Life Cycle Steps

Once the entity developing the life cycle profile identifies life cycle profile phases, the next step is to get validation of the life cycle profile phases from experts on the product itself. Validating the identified life cycle phases occurs by leveraging the product expert's high-level knowledge of the entire product life cycle.

With expert validation completed, the next step is identifying individual life cycle steps within each phase. A life cycle profile step is a specific event or procedure in that life cycle profile phase. Applying a higher resolution to the life cycle phases to identify life cycle steps ensures that the entity developing the life cycle profile can have a more in-depth analysis of the loading the product experiences during its life cycle. One can characterize a life cycle profile in many ways; four typical steps include a manufacturing and assembly step, a storage step, a transportation step, and an operational step.

Each life cycle step needs to catalog variations in these steps. Each variation could have a different effect on the overall product (e.g., longer duration, higher loading conditions, more cycles), and the life cycle profile would be less representative of the loads the product can experience over its lifetime. Examples of variations include, but are not limited to, extended or shortened storage times, multiple storage conditions and transportation procedures, rework following a manufacturing or assembly step, or repair and maintenance procedures during operation. Other examples of variation in operational steps are the same modes of operation occurring in different seasons and operating environments [23].

2.2.2.1 Life Cycle Profile Steps Before Beginning Operation

Figure 5 shows an example of two life cycle phases for a refrigerator motor inverter board before beginning operation. If the life cycle profile is long, split manufacturing, storage, or transportation steps into equal-duration cycles with the same conditions for each cycle. Each cycle covers a specific duration of time within the entire life cycle profile step. Note that life cycle phases before operation can combine manufacturing, storage, and transportation in each phase. However, one can also have only manufacturing steps in a phase and only storage or transportation steps in a phase, depending on the approach used for phase identification.

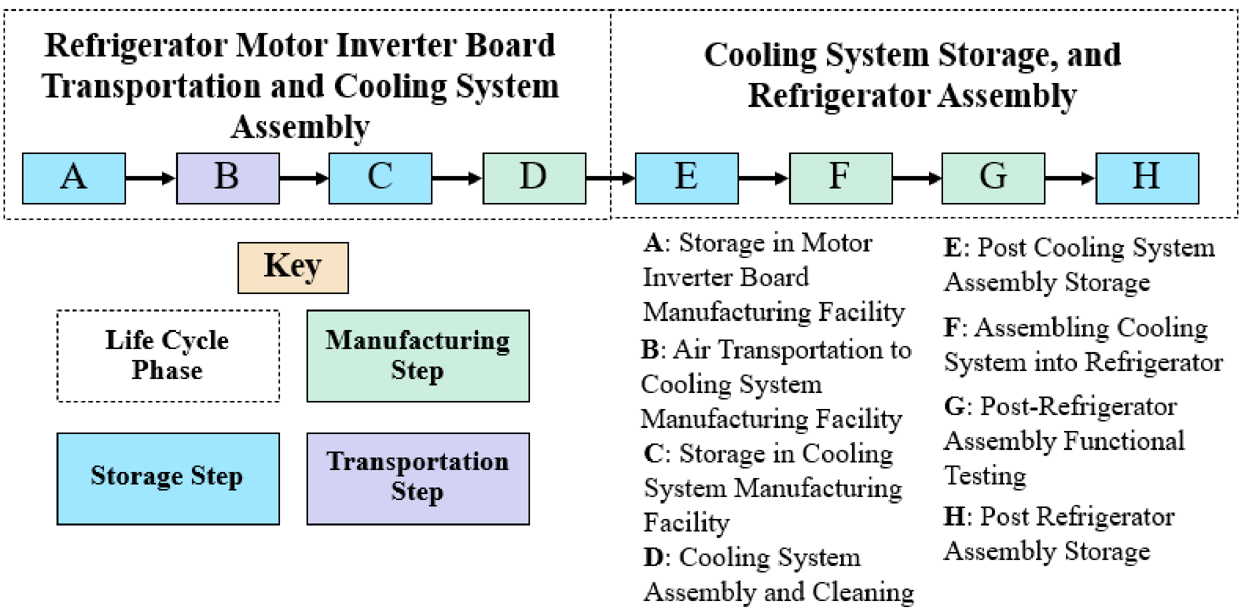

Figure 5: Examples of refrigerator motor inverter board life cycle phases and life cycle steps within each phase.

Manufacturing, storage, and transportation steps can have many variations that arise over their lifetime. For example, the refrigerator motor inverter board could undergo rework where certain board areas are exposed to elevated temperatures (e.g., 400°C) for a few seconds to induce localized solder reflow to fix a non-conforming part of the inverter board. Though rework is short relative to the product's lifetime, it still involves elevated temperatures, leading to localized thermal shock. As a result, rework should be considered nontrivial, especially considering that the components on this board could come from other boards that previously could have been affected by rework.

Figure 7 illustrates manufacturing and storage step variations that could include different combinations of storage locations, storage conditions, storage durations, and transportation methods. Each variation has its impact on the product as a whole. For instance, the product would experience storage at a port and transportation over the sea. As a result, it can get exposed to diurnal environmental cycling and corrosive atmospheres. When transported by air, the products could experience the effects of turbulence, diurnal cycling, and flight cycling.

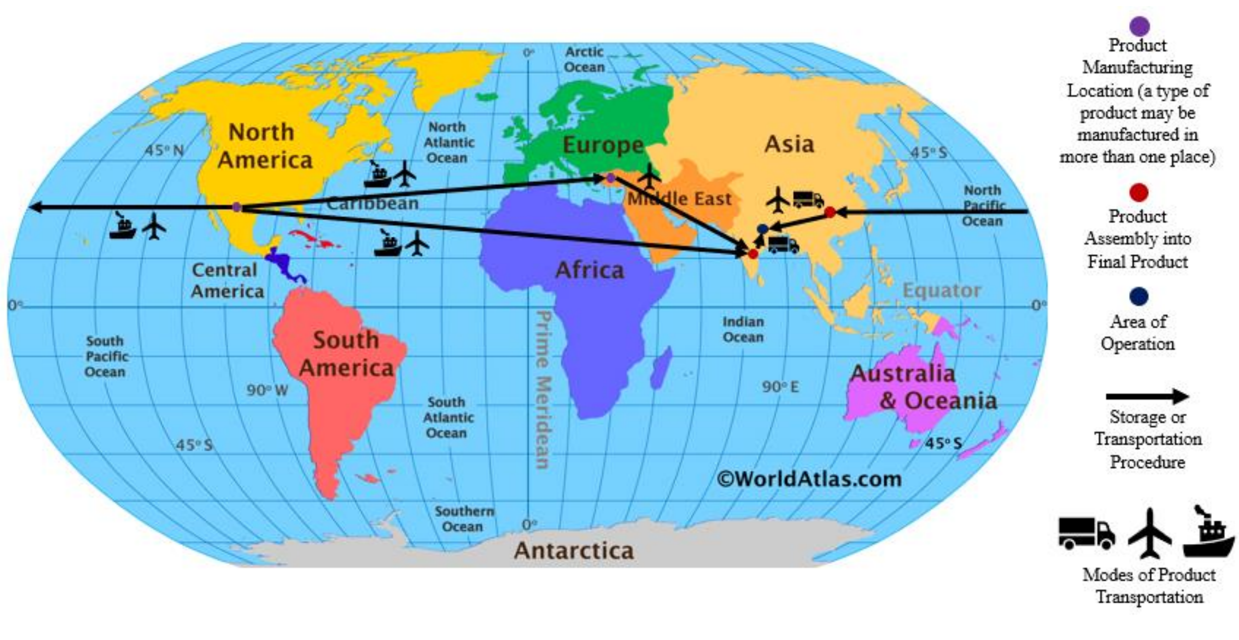

Figure 6: Multiple examples of product life cycle profiles begin at the same product manufacturing location and end at the same area of operation but with different intermediate locations. Note that the storage and

transportation procedures can have multiple options for modes of transportation.

2.2.2.2 Life Cycle Profile Steps During Operation

Multiple operational steps may arise over a product's lifetime. For instance, there is normal operation of the product. Normal operation could include multiple modes of operation. There are on/off steps for each mode of operation, where the product is turned on or off. As part of the operational steps, the product could experience idle days and downtime due to repair and maintenance.

Figure 7 shows an example of a refrigerator compressor's life cycle steps during operation. In this example, the refrigerator experiences pull-down following installation when the internal refrigerator cabinet temperature decreases from the ambient temperature to the desired refrigeration temperature. The compressor then continues a cyclical profile of compressor start-up, compressor running, compressor shut-down, and compressor-idle, corresponding to maintaining refrigeration temperature in the cabinet. If the refrigerator compressor remains idle for an extended period (e.g., due to a power outage, moving the refrigerator), the compressor would have to conduct pull-down again. Though the refrigerator pull-down step is not part of normal operation, it can occur multiple times over the product's lifetime. Consider the example of a refrigerator in a location that experiences daily power outages, leading to refrigerator pull-down every day. As a result, this variation in the life cycle profile can significantly impact the product's reliability.

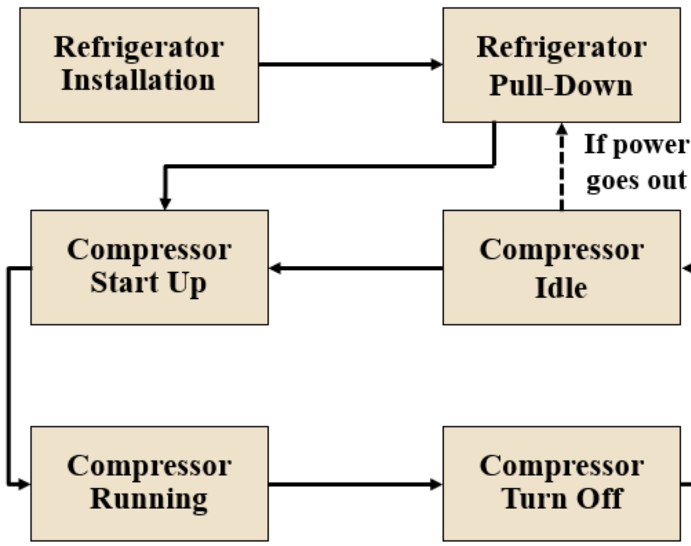

Figure 7: Example of life cycle steps in refrigerator compressor operation.

FIDES [23] provides an example of military applications in the form of life cycle profile development for external stores in multi-role fighter aircraft. FIDES' example includes three mission profiles for the aircraft, where each mission profile includes individual life cycle profile steps. Additionally, there is routine maintenance after every mission, and the aircraft remains idle for the rest of the day. For instance, one of the mission profiles, Patrol or Escort Mission, consists of the following life cycle steps:

- Wait on the ground
- Taxiing
- Climb
- Cruise (medium speed)
- Descent
- Taxiing

- Wait on the ground

2.2.3 Identifying, Estimating, and Modeling Life Cycle Loads

By extracting snapshots in each product life cycle stress profile step, one can generate a loading profile of the loads the product experiences across its lifetime. Military Standard 810 [15] lists potential loads in a life cycle profile in the context of environmental testing of military-grade products in various environments.

2.2.3.1 Characterizing and Estimating Life Cycle Stresses in Each Life Cycle Profile Step

Three methods for estimating life cycle loads are (1) numerical estimates of expected life cycle conditions, (2) qualitative categorization of the range that the expected life cycle conditions would fall within, and (3) cycle-counting algorithms to extract the cyclical behavior of data measured during prior product operation or environmental monitoring. The process for characterizing loads stated in Military Standard 810 [15] associated with military-grade products (gunfire shock, ballistic shock, pyroshock, and other loads) is beyond the scope of this paper.

2.2.3.1.1 Numerical Estimates of Life Cycle Loads

Numerical estimates of expected life cycle profile step loads originate from point estimates of loads imposed upon the product over the life cycle. Numerical estimates of life cycle loads can come from multiple sources, including simulation of operation, historical weather data, operational parameters, or standards and procedures for completing a particular life cycle step. Some examples of numerically estimable life cycle conditions include, but are not limited to, temperature, humidity, atmospheric pressure, vibration, thermal shock, rainfall, and solder radiation.

One example of numerically estimating the loads in a life cycle profile step is estimating the thermal loads the product experiences during solder reflow. Consider comparing the solder reflow profile as represented in Joint IPC/JEDEC Standard (J-STD) 20 [25] with an idealized numerical estimation of the solder reflow profile in Figure 8. Linearizing the curvature of the actual solder reflow profile simplifies future modeling of the solder reflow profile while still estimating the overall effects of the solder reflow profile.

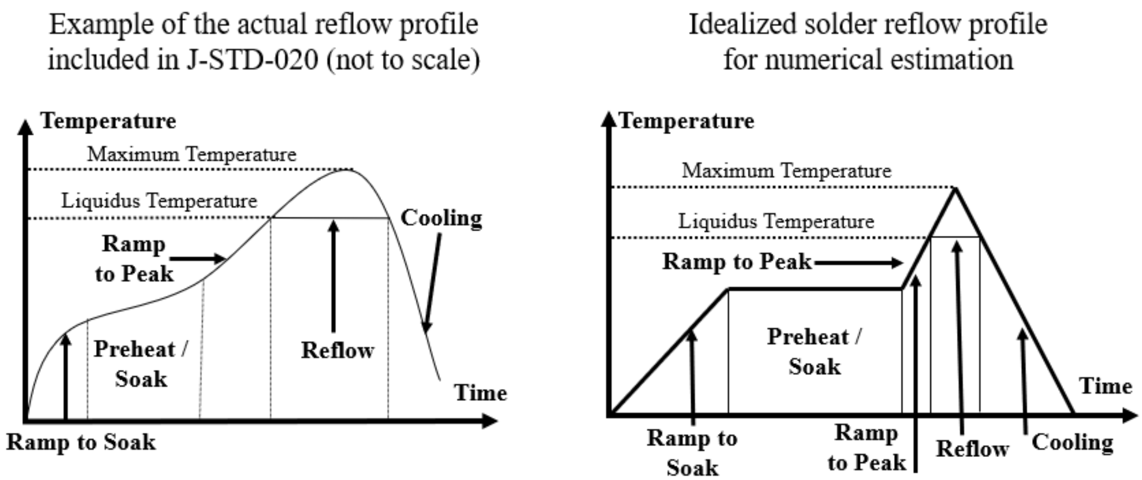

Figure 8: Solder reflow profile as provided in J-STD-020 (left). An idealized numerical estimate of solder reflow profile in J-STD-020 (right).

2.2.3.1.2 Qualitative Categorizations of Life Cycle Loads

Qualitative categorization applies in instances where the expected life cycle conditions are not estimable with a high degree of confidence, but the judgment of operating environments helps characterize the likelihood of multiple loading conditions. In such cases, one can characterize the impact of life cycle conditions as “low,” “medium,” or “high.” Table 4 includes examples of loads that could use qualitative categorization instead of numerical estimates.

Based on the qualitative categorization, the entity developing the life cycle profile can ignore the effects of “low”-categorized life cycle loads. The entity could then assume a representative loading value within the “medium”-categorized life cycle load boundaries. For “high”-categorized loads, the entity could assume multiple cycles of the limiting bounds, depending on the loads' severity. For example, consider qualitative categorization of salt fog conditions, representing corrosive environments’ effects. Using the salt fog categorizations in Table 4, as long as the product does not experience any corrosive atmospheres during a given life cycle step, one can characterize the effects of salt fog as “low.” As a result, one ignores the effects of salt fog in that life cycle step. If there is less than a 5%/hr exposure, then the effects of salt fog are categorized as “medium.” If there is a greater than 5%/hr exposure, the effects of the salt fog are “high.”

Table 4: Definitions and examples of qualitative categorizations for different life cycle conditions. Note: except for sand/dust, the inputs used to characterize the conditions stem from Military Standard 810 [15]. Additional note: the salt fog condition is representative of corrosive environments.

Life Cycle Profile Condition	**Condition Qualification**	**Low**	**Medium**	**High**
Fluid Contamination	The product experiences fluid contaminants for “XX” time.	<5 min	5 min – 3 hr	>3 hr
Fungus	The temperature is “XX” ℃ with relative humidity “YY” %RH for “ZZ” hours.	< 32℃ < 50% Any number of hours	> 32℃ > 50% < 4 hr	> 32℃ > 50% > 4 hr
Salt Fog	The product experiences a “XX” %/hr equivalent of salt fog.	0 % / hr	0-5% / hr	> 5% / hr

Life Cycle Profile Condition	Condition Qualification	Low	Medium	High
Sand/Dust	The effect of dust depends on the effect of “XX” % RH and how it relates to the critical relative humidity (CRH) for the dust in the environment in each life cycle profile step [26].	< 0.75 * CRH	Between 0.75*CRH and CRH	> CRH
Immersion	The product is immersed under “XX” m of fluid for “YY” min.	< 0.3 m < 30 min	< 0.3 m > 30 min	> 0.3 m Any number of minutes
Acidic Atmosphere	The pH of the rain is “XX.”	Between 6.5 – 7.5	Between 5.5 – 6.5	< 5.5
Icing / Freezing Rain	The product endures “XX” days of rain during freezing conditions each year. Assume freezing rain would only occur between November and April.	< 2.5 days	Between 2.5 – 10 days	> 10 days
Freeze / Thaw	The temperature reaches below and above freezing temperatures “XX%” of the year.	< 5%	Between 5-10%	> 10%

2.2.3.1.3 Cycle Counting of Life Cycle Loads

Numerical estimates and qualitative categorizations of life cycle conditions can come from empirical estimates from weather data, standards and procedures outlined for each life cycle profile step, and the experience of experts. Assuming tests were conducted on product samples to evaluate the effects of different procedures on the product, one can leverage data gathered from these tests to identify the loading profile and separate the life cycle profile into multiple cycles. Cycle counting algorithms apply to identifying individual cycles within the data and the number of times each cycle occurs.

An example of a cycle counting algorithm is the rainflow cycle counting algorithm, which Matsuishi and Endo first proposed in 1968 [27]. The algorithm analyzes the time history of loading and identifies cycles of that loading that exist within the entire time history. This algorithm then counts the number of times each type of cycle occurs over the time history of that load [28]. The manual interpretation for this procedure begins with rotating the chart of the time history of loading data 90° clockwise, as illustrated in Figure 9a. The algorithm identifies individual loading cycles by juxtaposing the image of raindrops flowing along each edge of the loading history, as represented in Figure 9b.

Many implementations of the rainflow algorithm utilize the American Society for Testing and Materials (ASTM) e1049-85's version [29], which evaluates the loading history three consecutive points at a time. In contrast, Matsuishi and Endo's algorithm [27] evaluates the loading history of two consecutive points simultaneously. However, the cycle ranges calculation methods remain the same between the two algorithm versions.

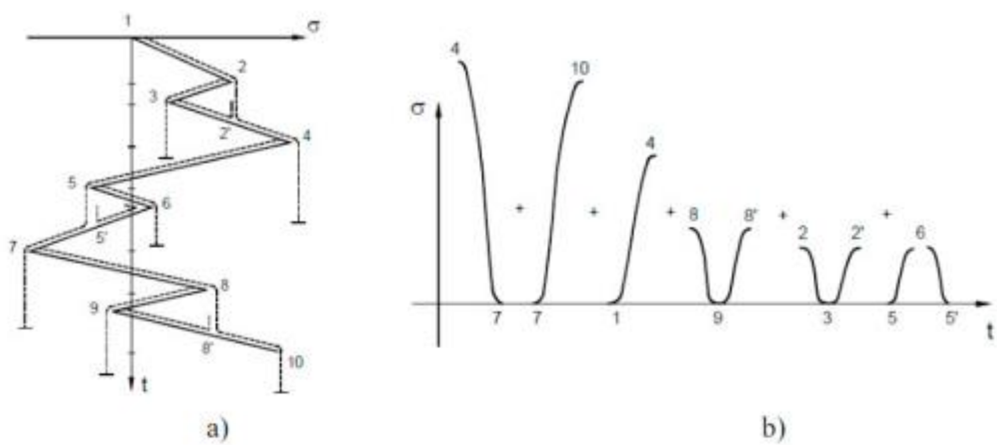

Figure 9: An example of the rainflow counting algorithm [30, 31] a) is the rotated loading time history for the product, and b) is the equivalent loading time history when separated into individual cycles.

2.2.3.2 Modeling Load Cycling Throughout the Life Cycle Profile

The next objective is to characterize the intensities of different loads in every life cycle profile step. Certain loads, such as temperature, relative humidity, atmospheric pressure, vibration, voltage, and current, could cycle during a life cycle step. One should account for the cycle's maximum and minimum loading values and the cycle duration within each step. Then, fit these parameters to the cycling profile shown in Figure 10 to capture cycling loads throughout each life cycle profile step. The cycle is assumed to be symmetric when considering cycling without extracted cycles to reference. This approach can account for both extreme load applications and sudden applications of elevated loads.

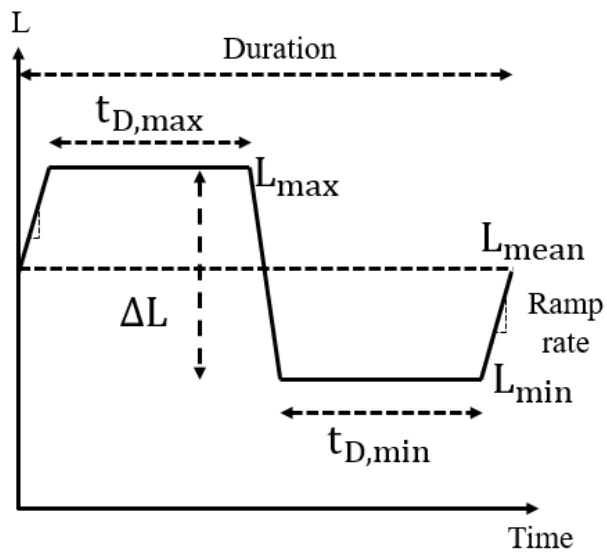

- L – variable for loading in cycle
- ΔL – range of loads in cycle
- $t_{D,max}$ – dwell time at maximum load
- $t_{D,min}$ – dwell time at minimum load
- Ramp rate – the magnitude of the slope for ramping between cycle extrema
- Cycle extrema: maximum and minimum load of cycle
- Duration – the total length of time of the cycle
- n_R – the number of instances of ramping between cycle extrema and mean (or vice-versa)
- D_f – the fraction of the cycle duration dwelling

Equation for calculating ramp rate (if not otherwise specified):

$$Ramp\ rate = \frac{n_R}{1 - D_f} * \frac{(L_{max} - L_{mean})}{Duration}$$

Figure 10: Example of a symmetric loading cycle and the different parameters governing the loading cycle.

The cycling profile demonstrated in Figure 10 has four instances of ramping from the mean to a cycle extremum (or vice-versa). Additionally, due to the symmetry assumption for the cycling profile, half the cycle duration is spent dwelling at a constant temperature. As a result, the given cycle profile has a ramp rate equation of:

$$\text{ramp rate} = \frac{4}{1-\frac{1}{2}} * \frac{(\mathrm{L_{max}} - \mathrm{L_{mean}})}{\text{Duration}} = 8 * \frac{(\mathrm{L_{max}} - \mathrm{L_{mean}})}{\text{Duration}}$$

It is important to note that one does not need to model the cycling for every load across the life cycle. Once the numerical estimates, qualitative categorizations, and identifying and counting life cycle condition characteristic cycles are complete, eliminate loads that do not impact the product in the life cycle profile. Consider the example of developing a product life cycle profile to choose a solder material; the possibility of chemical exposure or humidity would be low compared to the effects of temperature cycling, vibration and thermal and mechanical shocks. However, if the same entity is also interested in the effects of different loads on a board level, they need to account for the effects of humidity and chemical contamination on corrosion.

3 Determining Qualification Tests, Test Conditions and Durations, and Sample Requirements

Using knowledge from the life cycle profile and the potential failure mechanisms that can affect the component, one can determine the required qualification tests to assess the intended application requirements. With knowledge of the qualification tests, the test conditions and durations for each test stem from the life cycle profile. Using desired confidence levels and models for ensuring statistical significance in testing, one can also calculate sample lot requirements for each test. With all the qualification test requirements determined, product similarity can identify cases of redundant testing, further reducing the time and resources required to complete qualification while still accounting for intended application requirements. Each of these topics is in this section.

3.1 Determining Required Qualification Tests Using Failure Mechanism Risk Prioritization

Before completing failure mechanism risk prioritization, one needs to identify failure mechanisms that can affect the product over its lifetime. Failure modes, mechanisms, and effects analysis examine product physics-of-failure to determine the different processes by which a combination of loads (e.g., physical, electrical, chemical, mechanical sources) induce failures. These processes are known as failure mechanisms. While studying how failure mechanisms induce failure, the study of failure modes examines how one could observe or detect failure. Failure effects are the impacts and consequences of failure on the product, the surrounding system, or the infrastructure and environment in which the product is.

Using the life cycle profile for the product in the intended application and the results from failure modes, mechanisms, and effects analysis, the next objective is to determine the most important tests to run by prioritizing the failure mechanisms that can occur. The process for prioritizing failure mechanisms, as described by Kapur and Pecht [1], is outlined in Figure 11. Within this procedure, the first step of identifying potential failure mechanisms. Based on the life cycle loads found in the life cycle profile and the list of all potential failure mechanisms, one can evaluate the likelihood of different failure mechanisms causing product failures. After determining the failures that have the potential to occur, it is important to consider the severity of consequences of product failure based on how certain catastrophic types of failures would be to the product itself, the system the product is integrated into, and the infrastructure and environment the product is within.

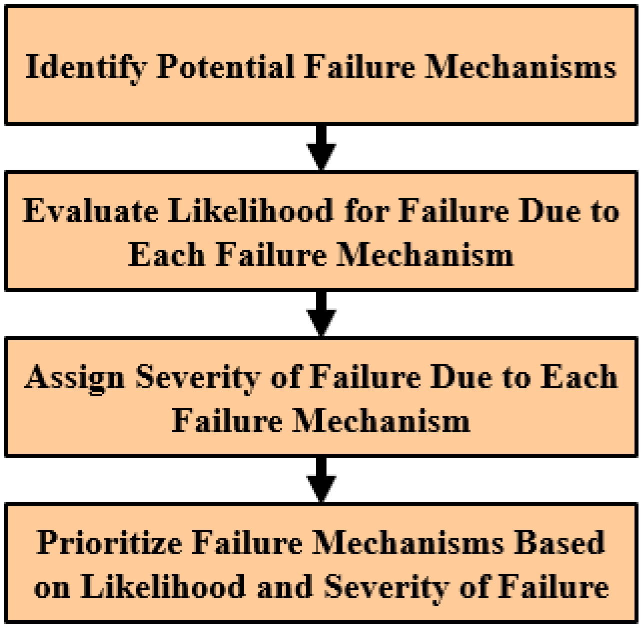

Figure 11: Procedure for prioritizing failure mechanisms based on the likelihood of failure occurring and the severity of the consequences of product failure [1].

After considering the likelihood of failure due to certain failure mechanisms occurring and the severity of the consequences of each product failure, choosing the qualification tests to run are based on the most likely and severe failure mechanisms. Each qualification test assesses a product's ability to function satisfactorily under the effects of various loadings (and, therefore, while being affected by different failure mechanisms.) Table 5 includes several examples of common qualification tests in component qualification and the purpose of each test.

Table 5: Examples of qualification tests and their purposes.

Qualification Test Example	**Purpose of Qualification Test**
High-Temperature Reverse Bias (HTRB) Test	Study product's stability and gate leakage current over time when there is no applied gate voltage [32].
High-Temperature Gate Bias (HTGB) Test	Examine drift of electrical parameters related to gate function due to gate oxide degradation [32, 33].
Intermittent Operating Life (IOL) Test	Observe product behavior and thermomechanical stress under switching operating conditions [34, 35, 36].
Temperature Cycling (TC) Test	Analyze component and solder interconnect resistance to the effects of extremely high and low alternating temperatures [37].
Unbiased Highly Accelerated Stress Test (UHAST)	Assess product moisture resistance under very humid and high-temperature conditions [37].
High Humidity High-Temperature Reverse Bias (H3TRB) Test	Evaluate the effects of humidity in combination with electrical and thermal loads (e.g., corrosion) [36, 38].
High-Temperature Operating Life	Determine the effects of bias conditions in high

Qualification Test Example	Purpose of Qualification Test
(HTOL) Test	temperatures over time [37].

3.2 Calculating Qualification Condition, Duration, and Sample Requirements

With knowledge of the loads experienced by the product over its lifetime and the critical failure mechanisms, one can calculate qualification conditions and duration requirements using acceleration factor models. Acceleration factor models are empirical or physical models of product degradation under different loadings. The ratio of the time-to-failure from the use conditions and durations to testing conditions and durations is known as the acceleration factor, which AF denotes. Table 6 includes some examples of acceleration factor models and their corresponding equations and descriptions of equation variables.

Table 6: Examples of acceleration factor models, their equations, and explanations of each equation's variables.

Acceleration Factor Model	Equation for Calculating Acceleration Factor	Variables in Equation
Norris-Landzberg's Modified Coffin-Manson Model (Temperature Cycling Acceleration Model) [39, 40]	$AF = \left(\frac{f_{use}}{f_{test}}\right)^{-m} * \left(\frac{\Delta T_{use}}{\Delta T_{test}}\right)^{-n} * e^{\frac{E_a}{k}\left(\frac{1}{T_{max,use}} - \frac{1}{T_{max,test}}\right)}$	use ~ each loading cycle in the product lifetime test ~ loading cycle used for testing $f = \frac{1}{\text{Duration}}$ ~ cycling frequency ΔT ~ maximum temperature minus the minimum temperature of each cycle

Acceleration Factor Model	**Equation for Calculating Acceleration Factor**	**Variables in Equation**
		E_a ~ activation energy k~ Boltzmann constant (= $1.381 * 10^{-23}\ \frac{J}{K}$) m, n ~ model constants
Boyko and Gerlach-Modified Generalized Two Stress Eyring Model (Temperature-Voltage Acceleration Model) [41, 42]	$AF = e^{\frac{E_a}{k}\left(\frac{1}{T_{max,use}}-\frac{1}{T_{max,test}}\right)} * \ln\left(\frac{V_{max,\ use}}{V_{max,test}}\right)^{\gamma_1} * \left(e^{\left(\frac{\ln(V_{max,test})}{k*T_{max,test}}-\frac{\ln(V_{max,use})}{k*T_{max,use}}\right)}\right)^{\gamma_2}$	T, V ~ temperature and voltage, respectively max, use ~ maximum value of each loading cycle in lifetime max,test ~ maximum value of each loading cycle used for testing E_a ~ activation energy k~ Boltzmann constant (= $1.381 * 10^{-23}\ \frac{J}{K}$) γ_1, γ_2 ~ model constants
Peck's Model (Temperature-Humidity-Voltage Bias Acceleration Model) [10, 41]	$AF = \left(\frac{RH_{use}}{RH_{test}}\right)^{-N} * \frac{f(V_{use})}{f(V_{test})} * e^{\frac{E_a}{k}\left(\frac{1}{T_{max,use}}-\frac{1}{T_{max,test}}\right)}$	use ~ each loading cycle in lifetime test ~ loading cycle used for testing RH ~ relative humidity f(V) ~ function of applied voltage E_a ~ activation energy k~ Boltzmann constant (= $1.381 * 10^{-23}\ \frac{J}{K}$) N ~ model constant

The “use” conditions and durations accounted for in the acceleration factor models come from the life cycle profile. Knowledge of model parameters (e.g., activation energies, model constants) should stem from regression analysis of data from historical testing of the same product or similar products. With this information, there are multiple approaches for determining test conditions and durations for testing.

One approach for determining qualification test requirements is to choose a test condition profile from test method standards, qualification standards, historical test conditions, or other sources. The test condition profile includes the conditions experienced during a single cycle/period within testing and the duration of that cycle/period of experiencing those conditions. With these conditions, one can calculate the required test duration (e.g., number of cycles or hours) so that testing satisfies the intended application requirements. Calculating the acceleration factor between each period of use and the period of testing, one approach for calculating the required testing duration is using the following equation:

$$\mathrm{N_{qual}} = \sum_{\mathrm{i=1}}^{\mathrm{C}} \frac{1}{\mathrm{AF_i}}$$

where:

- $\mathrm{N_{qual}}$ - required number of qualification cycles
- C – total number of cycles in product lifetime
- $\mathrm{i} \in \mathrm{C}$ – indexing through each cycle in the order of occurrence
- $\mathrm{AF_i}$ - acceleration factor for each cycle in the order of occurrence

Another approach for determining qualification test requirements is to select a desired total testing duration and determine test condition requirements accordingly. Depending on the nature of the acceleration factor model, this can become a multi-objective (Pareto) optimization problem, as the goal could be to select the most optimal test condition options that satisfy operational requirements. To assuage the complexity of the problem, one can choose certain testing profiles and duration, leaving many fewer free test condition parameters to optimize. Alternatively, one can make the problem more complicated by including the total testing duration and test profile parameters to all be free, requiring multi-objective optimization.

3.3 Calculating Test Sample Lot Size Requirements

The sample lot size is the number of samples that will undergo a qualification test. The sample lot size requirement is the number of samples that would need to undergo testing so that the results gathered from those sample components statistically represent the whole population of components to a certain confidence level. As a result, to meet these statistical requirements, one can choose to test all the samples required. The amount of testing required on each sample can decrease with the use of diagnostics and prognostics techniques (as discussed in Chapter 4). Calculating the sample lot size requirement applies to creating training, testing, and validation data sets for evaluating diagnostic and prognostic techniques.

One example of a sample lot size requirement estimation approach is by JESD47 [5]. JESD47 states that the number of samples required and corresponding failures allowable for each qualification test must satisfy the 90% confidence level of a Poisson exponential binomial distribution. JESD47 and U.S. Military Performance Specification 38535 [43] provide sample tables for determining requirements for varying allowable defects and confidence levels. The equation provided by JESD47 is:

$$\mathrm{N} \geq 0.5 * [\chi^2 * (2 * \mathrm{C} + 2{,}0.1)] * \left[\frac{1}{\mathrm{CDL}} - 0.5\right] + \mathrm{C}$$

N is the minimum required number of samples for verifying that the product would satisfy qualification requirements. C is the maximum number of defective samples allowable among the total samples. CDL is the desired confidence defect level. χ^2 is the Chi-squared distribution value for a 90% confidence level.

3.4 Using Product Similarity to Identify Redundant Testing

The theory behind similarity-based qualification begins with the determination that a given component/subsystem must undergo qualification that has enough shared characteristics with previously tested or examined components/subsystems. If this is a reasonable determination, it can be assumed that the new product would demonstrate similar behavior under the same test conditions and testing duration as the previously tested product [44].

One example of similarity-based qualification is the qualification family, which essentially extends the qualification results of one product to similar products if they have enough common characteristics. As described in AEC-Q101 [6], one of the major requirements for products or product lines to belong to the same qualification family is to utilize the same wafer fabrication technology (e.g., Power MOS, Zener, IGBT). They must also have been manufactured at the same wafer fabrication site. Additionally, the actual wafer fabrication process between products or product lines must have the same following attributes:

- Process flow

- Layout design rules
- Number of masks
- Cell density (if applicable)
- Lithographic process
- Doping process
- Passivation / Glassivation material and thickness range
- Oxidation process and thickness range
- Front/back metallization material, thickness range, and number of levels

Additionally, for products or product lines to belong to the same qualification family, AEC-Q101 requires sharing commonalities in the package assembly process. Firstly, all products or product lines must share the same package type (e.g., TO-220, SOT-23) and the same site of package assembly. Secondly, they must share all the following characteristics of the package assembly process:

- Leadframe base material
- Leadframe plating (internal and external to the package)
- Die attach material & method
- Wire bond material, wire diameter, and process
- Plastic mold compound (or other encapsulation material)

However, multiple studies have also related to the similarity-based qualification of products through simulation and intelligent computing. For example, Van Driel et al. [45] studied similarity-based qualification for ball grid arrays, using structural characteristics to demonstrate similar responses based on variations in these characteristics. The characteristics that van Driel et al. studied were die thickness, pad-to-body ratio, die-to-pad ratio, body size, body thickness, and substrate thickness. Van Driel et al. then simulated the product's behavior under thermomechanical loading while experiencing moisture diffusion with variations of the aforementioned structural characteristics. Using design of experiments and response surface modeling for optimization, van Driel et al. determined the structural similarity rules the products must meet to accept that qualification results of one set of ball grid arrays would apply to others.

Stoyanov et al. [46] examined using a self-organizing map to evaluate a quad flat package's ability to withstand the hot solder dip refinishing process. Original equipment manufacturers of high-reliability equipment use this procedure to reduce the potential for tin-whisker formation. The package characteristics that Stoyanov et al. used for similarity analysis were the die area to package thickness, die area to package area ratio, input/output cross-section to package volume, molding compound coefficient of thermal expansion, and molding compound thermal conductivity. The authors found that these package characteristics demonstrated product vulnerability via thermomechanical modeling. The self-organizing map clustered common characteristics between different packages to demonstrate the applicability of similarity-based qualification.

Stoyanov et al. [47] studied the historical data from 111 different tests from a test procedure conducted on each given sample electronic module. The authors operated on the assumption that a part would need to pass all these tests to be fully qualified. Separating the data streams corresponding to devices under test that survived the qualification test from those who failed, the authors used chi-squared goodness-of-fit statistical testing to compare histograms of failed device under test data to survivor data. The authors also noted another criterion for assessing if a test is redundant: if all the data histograms from the surviving devices are highly similar. If they are not similar, then that would imply that even though those devices survived, the responses can be nontrivially different from device to device, implying that qualification would still be required. Knowing the tests that would be most impactful on reliability assessment (i.e., the tests that have the most failures or deviation between survivors historically), these tests can be completed earlier in the qualification procedure. Expedited precipitation of failures due to these tests would demonstrate that the product cannot meet all qualification requirements earlier, reducing the required qualification time.

Leveraging the notion of product similarity, the goal is to identify other products similar to the product undergoing qualification. After identifying those other products, the next step is to examine previously reported qualification or testing conducted on those products. This information may be in publications in the literature, or it could be in different manufacturer-reported documents. Examples of these documents include process change notifications or product qualification reports. Table 7 provides an example of the qualification reported in a discrete IGBT process change notification. Note that the reported qualification provides a test method reference, testing conditions and durations, and the number of samples tested, and this can also be another reference along with qualification standards for information regarding the qualification procedure.

Table 7: An example of the qualification procedure reported in a discrete IGBT process change notification.

Test Conducted	**Test Method**	**Test Conditions**	**Test Duration**	**Number of Samples Failed**
High-Temperature Reverse Bias (HTRB)	JESD22-A108	Ambient temperature 150°C, 80% of maximum rated voltage	1008 hr	0/231
High-Temperature Gate Bias (HTGB)	JESD22-A108	Ambient temperature 150°C, 100% of maximum rated voltage	1008 hr	0/231
Intermittent Operational Life (IOL)	MIL-STD 750 Method 1037	On/Off Time: 60 s	15000 cycles	0/231

With the knowledge of the tests that the product has undergone and an adequate number of survivors among all tested samples, one can assume that a similar product can withstand those conditions. Using the notion of product similarity, one can also assume that the product undergoing qualification is qualified for those test conditions and durations. If the qualification requirements set by the life cycle profile are less than the conditions and durations from previously reported tests, then those tests can be considered redundant.

4 Implementation of Diagnostics and Prognostics Techniques to Component Qualification

Diagnostics techniques are methods for identifying anomalous behavior ("failure modes") at a given time using existing parameter values or analyzing the parameter trend leading up to that time. Prognostics techniques apply to forecasting and predicting future parameter behavior and the remaining time-to-failure. The goal of implementing diagnostics and prognostics techniques while conducting qualification tests is to identify anomalous behavior and estimate the time-to-failure under different loading conditions. Ancillary benefits for implanting diagnostics and prognostics techniques in qualification could include improving identifying limitations of the component/product in the application and making qualification more targeted to application requirements. Figure 12 provides the procedure for implementing diagnostics and prognostics techniques into product qualification discussed in this paper.

The concept of infusing diagnostics and prognostics techniques into qualification has been proposed before. Pecht et al. [48] and Pecht and Gu [49] proposed a fusion prognostics-based qualification approach that uses physics-of-failure models and qualification standards to identify failure criteria. The key difference between the approaches described in Pecht et al. [48] and Pecht and Gu [49], and the approach described in this thesis, is that this approach specifically highlights how to develop a qualification procedure and then how to apply diagnostics and prognostics techniques. Additionally, this approach includes examples of diagnostics and prognostics applications to analyze product behavior under loading.

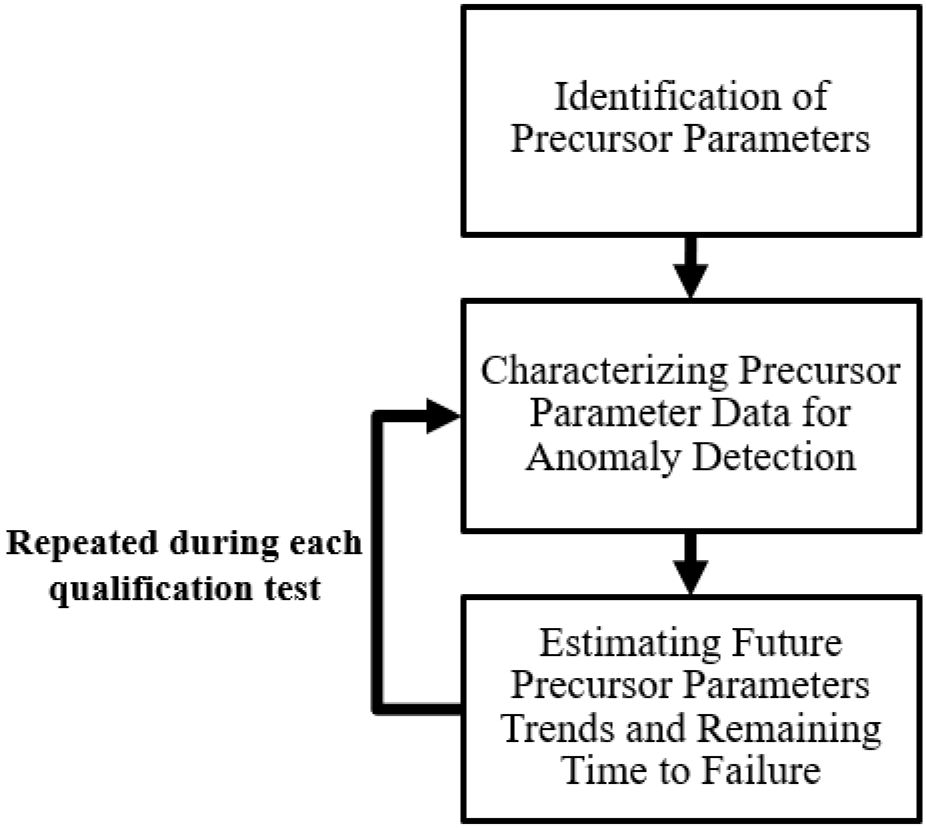

Figure 12: Example procedure for implementing prognostics-infused qualification discussed in this paper.

4.1 Determining Potential Precursor Parameters

Precursor parameters are operational and environmental characteristics to measure that track product behavior. Depending on the critical failure mechanisms for the product in the intended application, certain precursor parameters would be more sensitive to the effects of those failure mechanisms [50]. As a result, one can use precursor parameter measurements to evaluate product degradation due to different precursor parameters.

The goal of precursor parameter measurement is to identify failure precursors, which are events or series of events indicative of impending failure. Failure precursors are treated as failure modes, as they represent the way that failure is detected (which, when considering data-driven anomaly detection, parametrically.) Diagnostics techniques ultimately use precursor parameter measurements to identify failure precursors, and this procedure is also known as anomaly detection. Some examples of failure precursors include changes in precursor parameters, interactions between precursor parameters, and combinations of precursor parameters that could indicate an impending failure.

Table 8 provides examples of discrete IGBT and IGBT module precursor parameters and their corresponding failure effects.

Table 8: Examples of precursor parameters corresponding to the effects of different discrete IGBT and IGBT Module failure mechanisms.

<table>
<tr><th>Precursor Parameter (Discrete IGBT)</th><th>Corresponding Failure Effects</th><th></th><th>Precursor Parameter (IGBT Module)</th><th>Corresponding Failure Effects</th></tr>
<tr><td rowspan="4">On-State Collector-Emitter Voltage</td><td>Bond-Wire Fatigue [51]</td><td></td><td>Off-State Collector-Emitter Voltage</td><td>Bond-Wire Liftoff [52]</td></tr>
<tr><td>Die-Attach Degradation [51, 53]</td><td></td><td rowspan="2">On-State Collector-Emitter Voltage</td><td>Bond-Wire Fatigue [54, 55]</td></tr>
<tr><td>Solder Degradation [56]</td><td></td><td>Bond-Wire Liftoff [55, 57]</td></tr>
<tr><td>Latch-Up [53, 58]</td><td></td><td>High-Order Oscillatory Responses of Current and Voltage Transitions (Ringing)</td><td>Gate Oxide Degradation [59]</td></tr>
<tr><td>Gate Threshold Voltage</td><td>Gate Oxide Degradation
[51, 56]</td><td></td><td>Gate Current</td><td>Bond-Wire Defect [60, 61]</td></tr>
</table>

Precursor Parameter (Discrete IGBT)	**Corresponding Failure Effects**	**Precursor Parameter (IGBT Module)**	**Corresponding Failure Effects**
Miller Plateau Duration	Time-Dependent Dielectric Breakdown [62]	Junction Temperature	Bond-Wire Liftoff [57]
	Bond-Wire Liftoff [62]	Junction Temperature Ambient Temperature	Solder Fatigue [63]
Thermal Resistance	Solder Fatigue [64, 65]		Solder Fatigue [63]
Transconductance	Die-Attach Degradation [51]	On-State Resistance	Gate Oxide Degradation [66]
Transistor Turn-Off Time	Die-Attach Degradation [53]	Thermal Resistance	Solder Fatigue [64, 65]
	Latch-Up [53]	Transconductance	Bond-Wire Failure [67]
Collector Current	Latch-Up [53]		Chip Failure [67]

4.2 Characterizing Precursor Parameter Data for Anomaly Detection

After identifying the precursor parameters that track IGBT behavior, the next step is identifying the diagnostics techniques for anomaly detection. These diagnostics techniques identify discrete events that imply impending failure. Identification of these events can occur in real-time or using regression.

Three approaches for identifying specific events that imply impending failure are (1) supervised anomaly detection, (2) unsupervised anomaly detection, and (3) semi-supervised anomaly detection. Supervised anomaly detection uses predefined criteria for identifying healthy behavior and anomalous behavior. Unsupervised anomaly detection begins by assuming most of the data in an unlabeled dataset is healthy; any data points that are abnormal (anomalous) are considered unhealthy. Semi-supervised anomaly detection labels a certain selection of data within a dataset as healthy and classifies the rest of the data as healthy or unhealthy. Figure 13 provides examples of supervised, unsupervised, and semi-supervised anomaly detection.

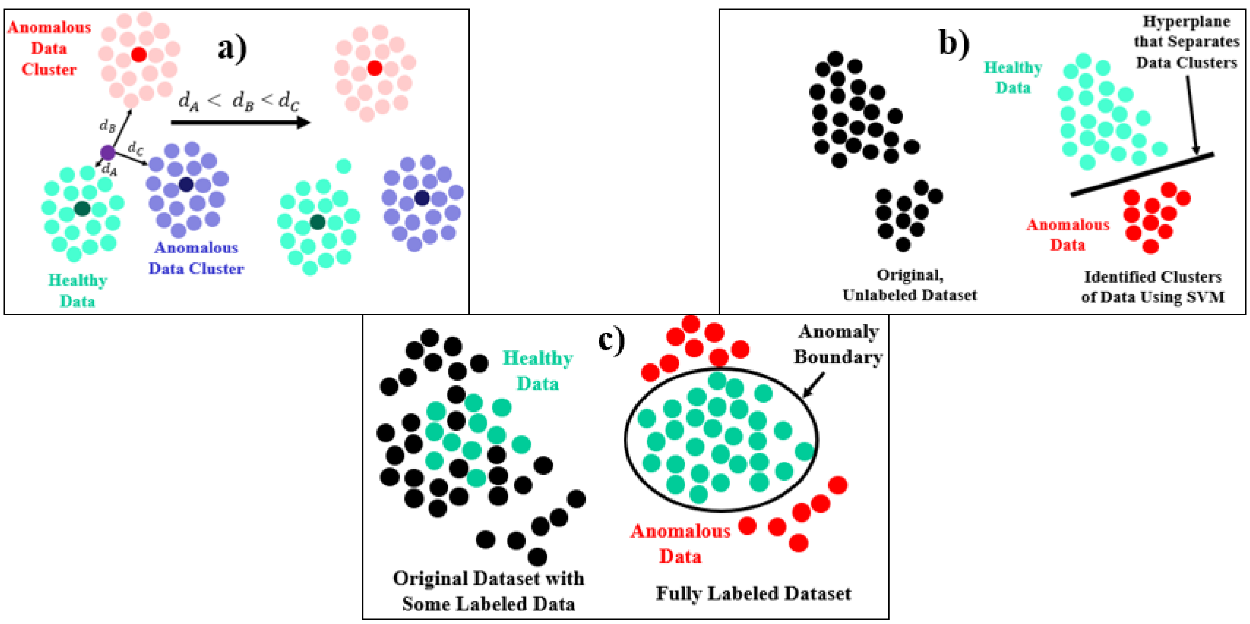

Figure 13: a) Example of K-nearest neighbor, a supervised anomaly detection technique. b) Example of a one-class support vector machine for unsupervised anomaly detection. c) Example of identifying an anomalous data boundary using Mahalanobis distance for semi-supervised anomaly detection.

Few studies have examined diagnostics techniques for discrete IGBTs. One study is that of Sutrisno et al. [68], who used K-Nearest Neighbor Classification (see [69] for more background on the method) with features found via a feature weight optimization algorithm to detect faults in 13/15 test samples correctly. Another study by Patil et al. [70, 71] investigated using the Mahalanobis distance of IGBT collector-emitter voltage and current from healthy data for in-situ anomaly detection of non-punch-through and field-stop IGBTs under highly accelerated electrical-thermal stresses. The authors could predict the onset of anomalous behavior between 57% and 77% of the time before failure occurred [70]. In other studies, Patil et al. [72, 73] also studied using robust covariance estimators to mitigate the effects of outliers on the sample mean and standard deviation estimation.

Multiple studies have examined diagnostics techniques for IGBT modules. For example, Ji et al. [63] observed a positive, linear correlation between the ambient temperature and IGBT junction-to-case thermal impedance, representing solder fatigue. In a separate study on identifying failure due to wire-bond faults, Ji et al. [55] determined that for the IGBT within their test, a loss of half the wirebonds corresponded to a 7% increase in the required on-state collector-emitter voltage. The authors also determined that if another wire were to fail, this would trigger irreversible IGBT module failure. Liu et al. [74] used a prediction interval-based approach to estimate online IGBT module degradation, characterizing degradation into three levels. A Mahalanobis distance estimator separates Level 1 from Level 2, and any data points beyond the 0.9999 bounds fall into Level 3. Lu et al. [75] used principal components analysis and K-means clustering for anomaly detection, applying some labeled healthy data to identify unhealthy data.

4.3 Estimating Future Parameter Trends and Remaining Time-to-Failure

Once diagnostics techniques identify data anomalies indicative of impending failures, the next step is to evaluate the time remaining before failure occurs. This process occurs through the use of prognostics. In theory, a data-driven, model-based, or hybrid approach would yield estimations of the remaining time-to-failure.

Data-driven prognostics-infused qualification requires large quantities of data from various sources, and it leverages data analytics approaches like machine learning to estimate future parameter trends. These methods are independent of the system and its failure behavior. Model-based prognostics-infused qualification utilizes pre-identified mathematical failure models to determine the degradation rate and therefore remaining time-to-failure based on the loads applied to the system [76]. A hybrid approach to prognostics utilizes both data-driven and model-based prognostics. One example of a hybrid approach is when a failure model influences the results using data-driven approaches.

Several discrete IGBT and IGBT module prognostics studies have used particle filters to estimate degradation paths of different parameters [75, 77, 78]. The particle filter solves for the Bayesian posterior distribution by approximating each Bayesian prior distribution as a discrete probability density function and solving the integral form of Bayes theorem [79, 80] as a series of summations [80]. The prior distributions influence the weights associated with different distribution samples ("particles"), and the sample weights influence the final estimation of remaining time-to-failure. Figure 14 demonstrates how a particle filter works.

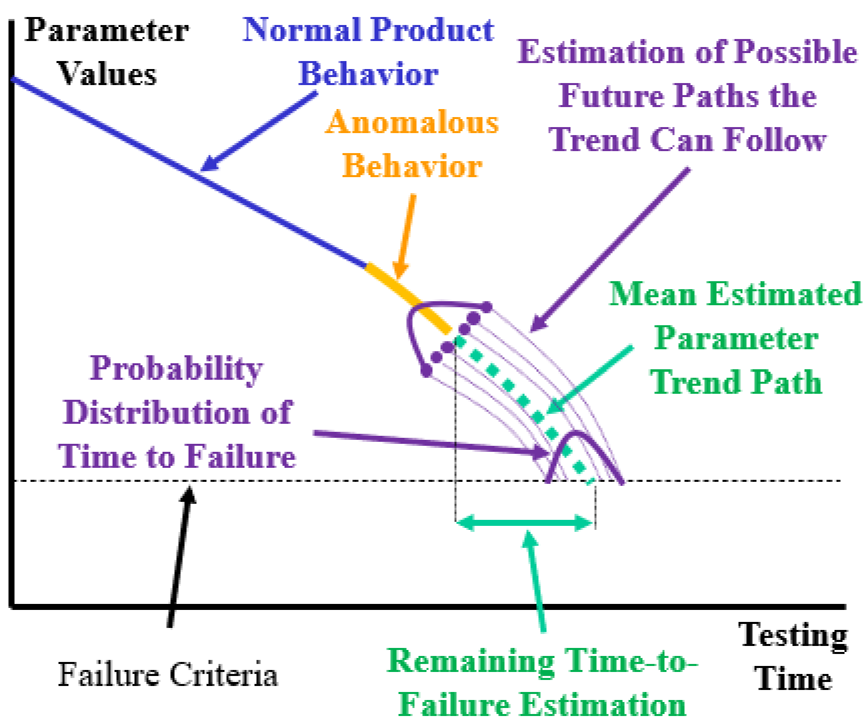

Figure 14: Example particle filter used to estimate remaining time-to-failure based on a given precursor parameter trend and a prior distribution.

In the study of prognostics for discrete IGBTs, continuing the work involving IGBT anomaly detection using Mahalanobis distance measurements [70], Patil et al. [77] also investigated using a particle filter for estimating the time to failure for both non-punch through and field-stop IGBTs. The particle filter approach used a model based on the collector-emitter voltage when the IGBT was in the forward operating mode, and it was able to predict the remaining useful life with an approximate underestimation error of 20%. Sreenuch et al. [81] developed an approach to estimate the IGBT remaining useful life using a Monte Carlo degradation path estimation based on the collector-emitter voltage of the component. Assuming possible paths followed a Poisson distribution, the algorithm proposed found the mean predicted remaining useful life to be the most accurate. Additionally, assuming the paths followed an exponential model, the algorithm found that the median predicted remaining useful life was the most accurate. Ali et al. [82] investigated using maximum a posteriori probability and Bayesian inference in conjunction with Gaussian Process Regression to estimate remaining useful life. The precursor parameter used in this analysis was the on-state collector-emitter voltage.

Regarding IGBT module prognostics, Lu et al. [75] work using a particle filter to estimate remaining useful life with failure caused by bond-wire liftoff and power cycling conditions. The authors leveraged a power-law polynomial failure precursor model and sampling importance resampling to guide the particle filter approach. Another example is Hu et al. [78] estimated wirebond remaining useful life during power cycling using a particle-based marginalized resample-move algorithm and Miner’s rule. The particle-based algorithm estimates the current crack length and other required values for remaining useful life estimation, and Miner’s rule determines the number of cycles the wirebonds can withstand before failure. Alghassi et al. [83] used an IGBT module's time-dependent neural network failure model to act as an overall health indicator. The time delay neural network uses collector-voltage drift as a health indicator for wirebond liftoff. Then, the algorithm separates the overall degradation curve of the IGBT into individual degradation states that the IGBT would experience over time. Using the time delay neural network failure model to estimate the total duration of each future degradation phase, summing these phase durations results in the remaining useful life of the product.

4.4 Using Historical Data for Diagnostics and Prognostics Technique Evaluation

As noted by Stoyanov et al. [47], a common practice in the electronics industry is to archive the measurements of product behavior during previously conducted qualification and life tests on different products. Historical test data is applicable for completing similarity-based qualification to remove redundant tests that products have not failed before. However, offline analysis of historical qualification data is also applicable for assessing the ability of diagnostics and prognostics techniques for anomaly detection and remaining time-to-failure estimation. Recall from Section 3.4 that similar products would demonstrate similar behavior under the same test conditions and testing duration [44]. This would also imply that trends observed in historical data of previous products would also apply to new products that are similar.

Continuing their study of the results of 111 historical tests conducted on each given sample electrical module, Stoyanov et al. [47] examined the use of support vector machines on the data gathered from 27 tests that were most likely to precipitate failures. Using just the data from these tests, the authors could accurately predict if failures would occur in tests further on in the qualification procedure. The accurate predictability of whether the product would survive or fail the remaining qualification test can provide huge cost and time savings for completing the qualification of each electronic module. The authors note that if the approach predicts that failures will occur, that product's qualification continues to validate the result.

One example of the application of historical data and product similarity is by Wang et al. [84]. The authors used an assumed representative set of historical run-to-failure data to identify each product's form of the degradation model. Maintaining a library of these degradation model forms, the approach uses distance-based algorithms to represent the similarity of behavior between each degradation model and the test data results. Solving for the remaining useful life by applying each degradation model, the distances representing similarity contribute to the weighting function. The estimation of the remaining useful life is the weighted sum of all degradation model remaining useful life estimations.

Maio et al. [85] sought to estimate the remaining useful life for a given component or structure. The authors noted that experimenters might take very few measurements at predefined points during testing to lower computation time and costs associated with the testing procedures. As a result, the authors developed a framework that uses a fuzzy-based similarity analysis methodology to predict the remaining useful life when the test data reveals a new degradation pattern. The new degradation pattern is compared to a library of degradation-to-failure patterns from historical data to generate the remaining useful life estimation. The authors applied a Gaussian membership algorithm to weight the point-wise L1 Euclidean distance between each known degradation-to-failure pattern point and the corresponding test pattern point. The actual remaining useful life estimation was then the sum of the remaining useful life estimate from each pattern multiplied by each corresponding weight.

5 Case Study: Discrete IGBT Qualification for a Hypothetical Refrigerator Application

A hypothetical home appliances company experienced refrigerator failures over several years. The timeline of refrigerator failures reveals that most failures occurred in operation. Further analysis of these refrigerator failures revealed that the discrete IGBTs within the refrigerator motor inverter boards failed. The inverter board controls the refrigerator compressor, and the refrigerator compressor is responsible for circulating the vaporized refrigerant throughout the system. Failure analysis of the discrete IGBTs demonstrated the presence of burn marks on the gate region of the IGBT die surface caused by high transient voltages. Figure 15 is an example of a failure analysis conducted by the home appliances company on a decapsulated discrete IGBT.

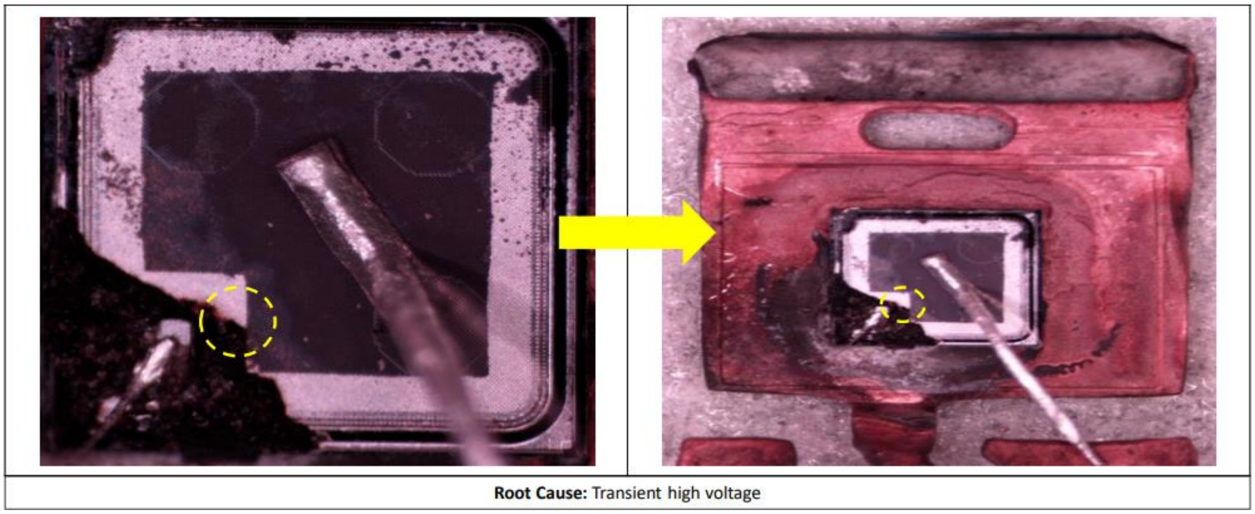

Figure 15: Example of decapsulated discrete IGBT failure analysis conducted by the home appliances company.

When considering approaches for eliminating these IGBT failures, one tangible course of study is the applicability of defect precipitation techniques (e.g., screening, burn-in) to eliminate defective IGBTs before being implemented into the refrigerator motor inverter board. However, before considering defect precipitation techniques, one should consider whether these discrete IGBTs can meet the application requirements for ten years (the desired refrigerator lifetime.) Having an approach for assessing the IGBT's ability to meet application requirements can also enable parts selection management should other IGBTs be considered for this application and requalification of the IGBTs if a product change occurs within either the IGBT or the electronic product it is being implemented into (i.e., the refrigerator motor inverter board.) As a result, CALCE, in conjunction with the home appliances company, used the approach described above for completing IGBT qualification.

The IGBTs in the refrigerator motor inverter board are Infineon IKD06N60R trench-stop, surface-mounted, discrete IGBTs [86] with an integrated anti-parallel diode within the package. A summary of the ratings for the Infineon IKD06N60R IGBT is in Table 9. The trench-stop nature of the Infineon IKD06N60R IGBT involves a trench-gate metal-oxide field-effect transistor (MOSFET) and a field-stop bipolar junction transistor (BJT). The trench gate MOSFET contains trenches that conduct currents vertically from the gate to the drift region of the IGBT, thereby eliminating parasitic resistances compared to planar gate technologies. The field-stop BJT contains a smaller drift region than non-punch-through IGBT technologies, a lower turn-off current, and lower losses than punch-through IGBT technologies. The antiparallel diode within the IGBT structure enables reverse-bias operation, which would be particularly useful in applications that require a bidirectional switch.

Table 9: Summary of power and environmental ratings for Infineon IKD06N60R [86].

Power Ratings

	V_{CE}	**V_{GE}**	**I_C**	**I_C**	**I_{CP}**	**I_F**	**I_F**	**P_D**
Temperature Condition (°C)			**25**	**100**		**25**	**100**	**25**
	600	20	12	6	18	12	6	100

Environmental Ratings

T_J	**T_J**	**T_{St}**	**T_{St}**	**T_{Sld}**	**MSL**
Min	Max	Min	Max	Max	
-40	175	-55	150	260	1

V_{CE} – Collector-Emitter Voltage (V)

V_{GE} – Gate-Emitter Voltage (V, ±)

I_C – Collector Current (A)

I_{CP} – Pulsed Collector Current (A)

I_F – Diode Continuous Forward Current (A)

P_D – Maximum Power Dissipation (W)

MSL – Moisture Sensitivity Level

T_J – Junction Temperature (°C)

T_{St} – Storage Temperature (°C)

T_{Sld} – Soldering Temperature (°C)

Figure 16 includes pictorial representations of different discrete IGBT technologies, particularly planar gate punch-through (PT), planar gate non-punch-through (NPT), and trench-stop IGBTs.

Table 10 highlights key differences between punch-through, non-punch-through, and field-stop IGBTs. In punch-through IGBTs, carriers are injected at high rates to obtain a low on-state voltage, thereby prescribing the high emitter efficiency requirement. The buffer layer limits the number of holes injected into the drift region and absorbs holes during turn-off, curtailing the tail currents observed during turn-off, leading to a low carrier lifetime. In non-punch-through IGBTs, the IGBTs have low carrier concentrations (in direct opposition to punch-through IGBTs), but it also requires a larger drift region to accommodate the triangular electric field that forms during the blocking condition. This larger drift region can result in static and dynamic losses. Field-stop IGBTs overcome the triangular electric fields in non-punch-through IGBTs while enabling low carrier concentrations and a high carrier lifetime. This, in turn, contributes to field-stop IGBTs potentially having lower dynamic losses (an improvement over non-punch-through technologies) and a lower on-state voltage (an improvement over punch-through technologies) [87]. Because non-punch-through IGBTs have equal forward and reverse breakdown voltages, they are best suited for alternating current (AC) applications, where the device must support large voltages in either direction. Punch-through and field-stop IGBTs, in contrast, have smaller drift regions than the non-punch-through IGBT, implying that the device does not have large breakdown voltages. This makes punch-through and field-stop IGBTS more suited for direct current (DC) applications, where electricity flow is assumed to flow primarily in one direction [88].

The difference between planar and trench gate technologies is that trench gate technologies have a lower on-state voltage, can better manage the effects of latch-up, and have a higher breakdown voltage than planar technologies [89]. The trench gate structure consists of an accumulation layer along the trenches that connects the n+ source to the n- drain and improves the conduction of electrons into the drift region [88, 90, 91].

Table 10: Comparison of characteristics of punch-through, non-punch-through, and field-stop discrete IGBT technologies [87, 92].

	PT-IGBT	**NPT**	**Field Stop**
P-Emitter	High efficiency	Low efficiency	Low efficiency
N*-Layer	Thin	Medium	Thin
Additional N-Layer	Highly doped buffer layer	None	Weakly doped buffer layer
Purpose of Additional N-Layer	Reduce emitter efficiency Stop electrical field	N/A	Stop electrical field
Carrier Lifetime	Low	High	High

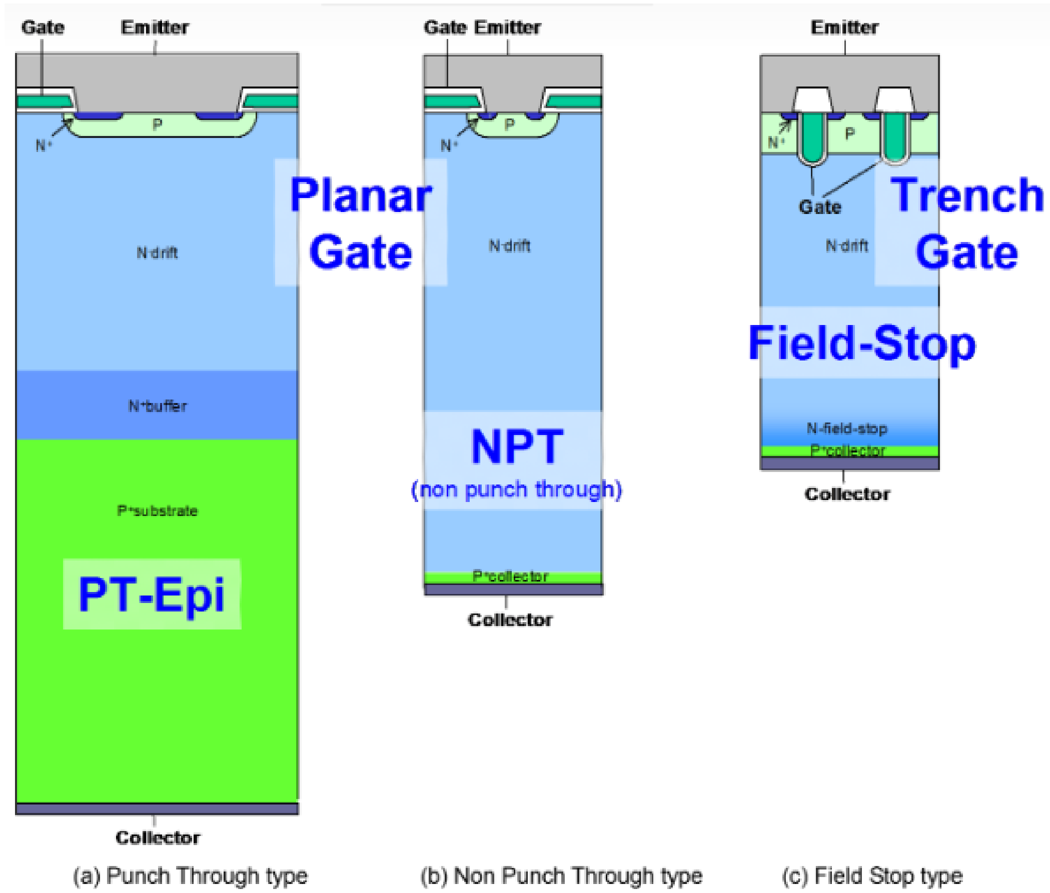

Figure 16: Comparison of different discrete IGBT technologies [93]. Note that Figure 16c represents the structure of Infineon IKD06N60R and that the accumulation layer on the trench gate structure is the white perimeter of the gate.

5.1 Evaluating the Life Cycle Profile for the Discrete IGBT

Discussions with the home appliances company revealed that the main types of loading the product experiences before operation are temperature-related loads (e.g., elevated temperatures, temperature cycling.) During operation, the loads that the product experiences are temperature-related loads and electrical loads. Consequently, the life cycle profile for the discrete IGBT focuses on cataloging these types of loads. Unless otherwise stated, each of the load cycle profiles described in the below life cycle profile assumes the profile from Figure 10. Additionally, unless otherwise stated, assume that only one cycle of the loads occurs in a given life cycle step.

5.1.1 Loading Experienced Before Refrigerator Operation

Before product operation, most of the temperature-related loads arose from temperature cycling. This loading is experienced within the storage and transportation during refrigerator assembly and then within storage and transportation to the customer site. A process flow of the phases and steps within the storage and transportation during refrigerator assembly are in Figure 17.

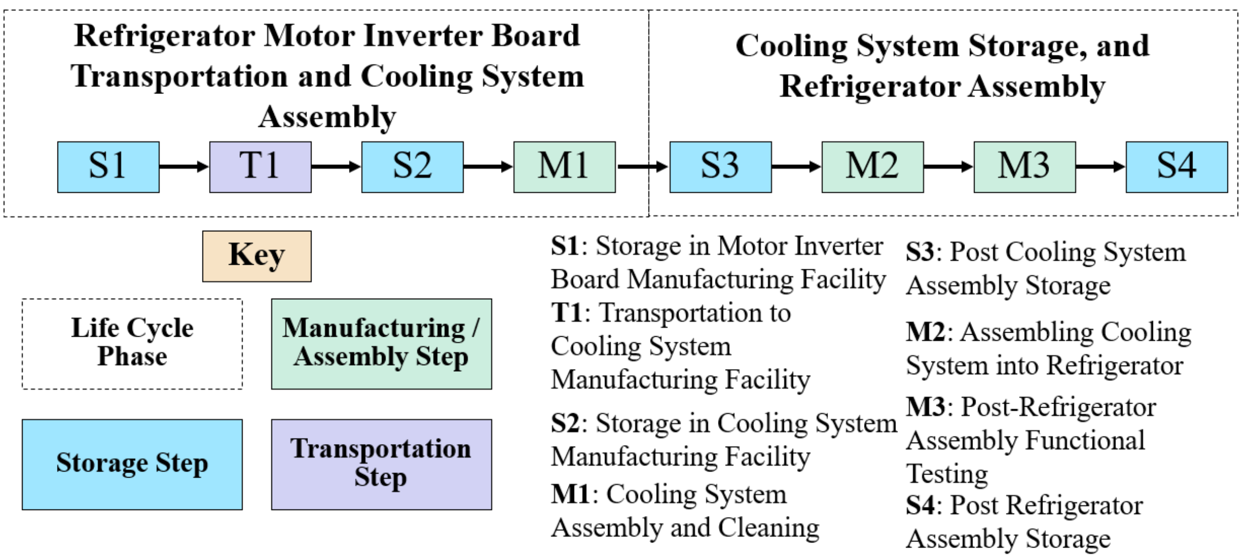

Figure 17: Life cycle phases and steps during refrigerator assembly storage and transportation.

The temperature cycling profiles experienced in each of these life cycle phases and steps are in

Table 11. Note that no temperature cycling is assumed in each of the manufacturing/assembly steps: cooling system assembly and cleaning, assembling the cooling system into the refrigerator, and post-refrigerator assembly functional testing. In these life cycle steps, it is assumed that there

is a fewer than 5°C temperature range, and this assumption stems from the fact that these steps occur in thermostatically controlled manufacturing environments for short enough duration so that the products also do not experience diurnal environmental temperature cycling effects. In contrast, though storage is assumed to occur in a thermostatically controlled environment, since storage can last days and weeks, one cannot ignore diurnal environmental temperature cycling effects, and hence a 10°C-temperature range is assumed. Additionally, due to the short duration and nature of functional testing, the electrical loads applied to the product are assumed to be trivial with respect to the electrical loads and duration of electrical loading experienced by the product over operation.

Additionally, note that storage and transportation steps include multiple possibilities, noted as “A,” “B,” or “C.” In the case of storage, option “A” implies storage for two weeks in that life cycle step, while option “B” implies storage for a total of 2 months in that life cycle step. Temperature cycling during these periods is split into six-hour cycles, and thus each step includes multiple cycles. In transportation, option “A” implies ground transportation, which lasts up to 2 days in thermostatically uncontrolled environments. During ground transportation, extreme temperature swings account for changes in climatic conditions during transportation from one location to another. Option “B” implies sea transportation, which can last up to 2 months. Like in ground transportation, extreme temperature cycling is assumed to account for changes in climatic conditions in thermostatically uncontrolled environments. Option “C” is air transportation, where cycling in high-altitude environments dominates. This approach assumes that transportation would take up to 12 hours in a single life cycle step.

Table 11: Profiles of temperature cycling experienced during storage and transportation of the refrigerator assembly.

Steps in the Procedure	T_{min} (°C)	T_{max} (°C)	T_{mean} (°C)	ΔT (°C)	Calculated Ramp Rate	$t_{D,max}$ and $t_{D,min}$	Duration	Number of Cycles
S1A	20	30	25	10	6.67 °C/hr	1.5 hr	6 hr	56
S1B	20	30	25	10	6.67 °C/hr	1.5 hr	6 hr	240
T1A	-6	30	12	36	24 °C/hr	1.5 hr	6 hr	8
T1B	-6	30	12	36	24 °C/hr	1.5 hr	6 hr	72
T1C	-50	-40	-45	10	24 °C/hr	1.5 hr	6 hr	2
S2A	20	30	25	10	6.67 °C/hr	1.5 hr	6 hr	56
S2B	20	30	25	10	6.67 °C/hr	1.5 hr	6 hr	240
M1	N/A							
S3A	20	30	25	10	6.67 °C/hr	1.5 hr	6 hr	56
S3B	20	30	25	10	6.67 °C/hr	1.5 hr	6 hr	240
M2	N/A							
M3	N/A							
S4A	20	30	25	10	6.67 °C/hr	1.5 hr	6 hr	56
S4B	20	30	25	10	6.67 °C/hr	1.5 hr	6 hr	240

Following storage and transportation during refrigerator assembly, the next life cycle phases and steps for the discrete IGBT life cycle profile are those associated with storage and transportation en route to the customer site. Figure 18 includes the life cycle phases and steps within the process of refrigerator storage and transportation en route to the customer site. As with the storage and transportation during refrigerator assembly, it is assumed that the temperature-related effects experienced by the product are due to temperature cycling.

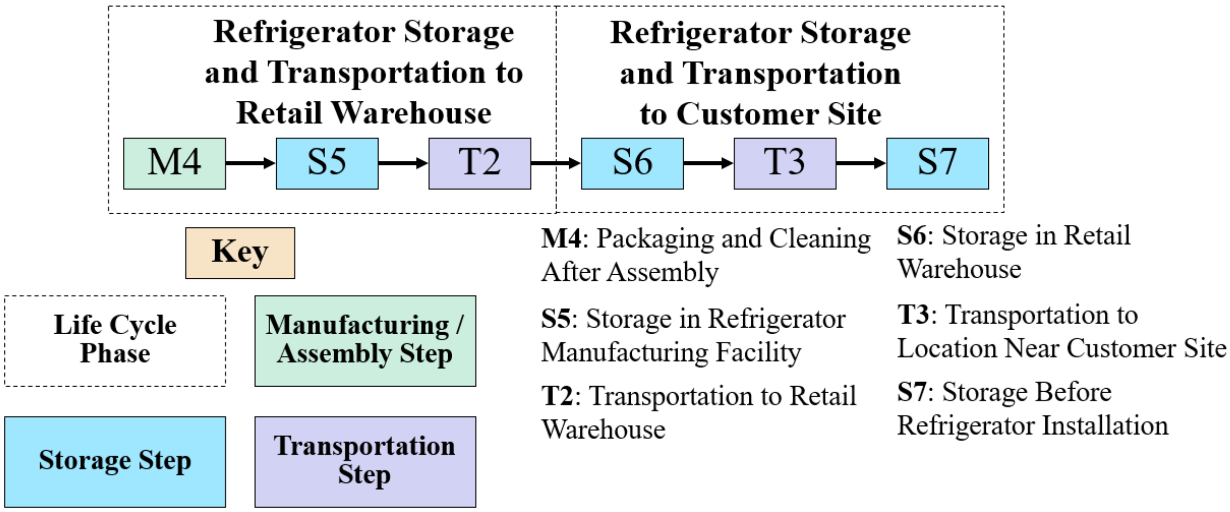

Figure 18: Life cycle profile phases and steps during storage and transportation en route to the customer site.

Table 11 apply to the profiles in

Table 12. Note that transportation from the retail warehouse to the customer site is assumed to occur exclusively using ground transportation, hence why “T3: Transportation to Location Near Customer Warehouse” only assumes the option of ground transportation. Also, once the refrigerator is near the customer site, it is assumed that any storage there would take a day or less before installation of the refrigerator.

Table 12: Profiles of temperature cycling experienced during storage and transportation en route to the customer site.

Steps in the Procedure	T_{min} (°C)	T_{max} (°C)	T_{mean} (°C)	ΔT (°C)	Calculated Ramp Rate	$t_{D,max}$ and $t_{D,min}$	Duration	Number of Cycles
M5	N/A							
S5A	20	30	25	10	6.67 °C/hr	1.5 hr	6 hr	56
S5B	20	30	25	10	6.67 °C/hr	1.5 hr	6 hr	240
T2A	-6	30	12	36	24 °C/hr	1.5 hr	6 hr	8
T2B	-6	30	12	36	24 °C/hr	1.5 hr	6 hr	72
T2C	-50	-40	-45	10	24 °C/hr	1.5 hr	6 hr	2
S6A	20	30	25	10	6.67 °C/hr	1.5 hr	6 hr	56
S6B	20	30	25	10	6.67 °C/hr	1.5 hr	6 hr	240
T3A	-6	30	12	36	24 °C/hr	1.5 hr	6 hr	8
S7	-6	30	12	35	6.67 °C/hr	1.5 hr	6 hr	4

5.1.2 Loading Experienced During Refrigerator Operation

The life cycle steps that occur during product operation are pictorially demonstrated in Figure 19. The combination of the compressor starting up, running, turning off, and staying idle is now referred to as "normal operation." Normal operation corresponds to maintaining the desired cabinet temperature over time. Refrigerator pull-down is the process by which the refrigerator rapidly brings the internal cabinet temperature to the desired temperature from a higher temperature (e.g., the ambient temperature outside the refrigerator cabin.) This procedure occurs when the refrigerator is installed and turned on or when refrigeration is interrupted for extended periods (e.g., while moving the refrigerator, power outages.) As a result, it is assumed that this refrigerator pull-down occurs once a day to better represent the needs of the home appliance company's customers in regions with unstable power grids. During refrigerator operation, both temperature-related loads and electrical loads affect the discrete IGBTs in the refrigerator motor inverter boards, and therefore estimations of both types of loading are in Sections 5.1.2.1 and 5.1.2.2.

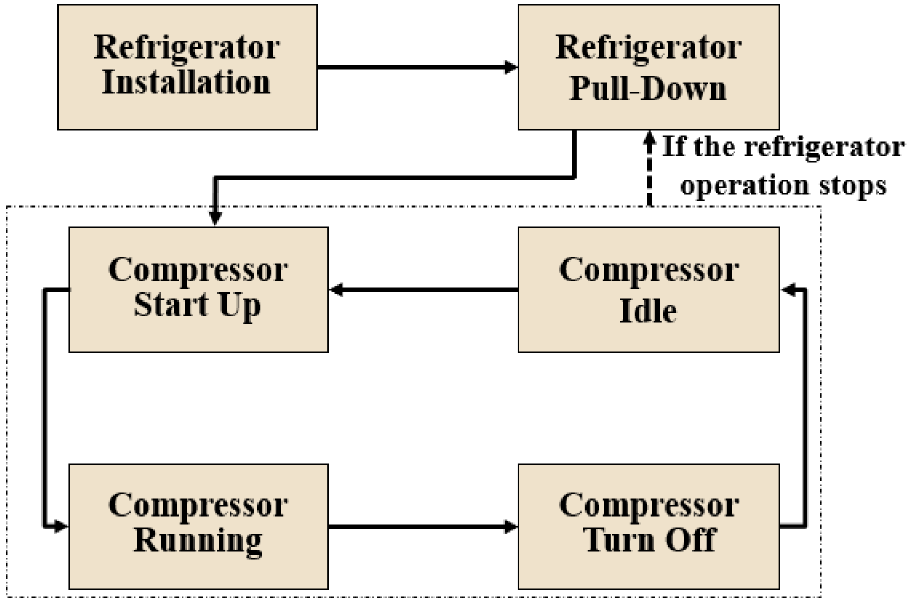

Figure 19: Life cycle steps experienced by the product during product operation. Note that the combination of compressor start-up, running, turn-off, and compressor-idle make up "normal operation."

5.1.2.1 Estimation of Temperature-Related Loads in Product Operation

Unlike the temperature cycling assumed before operation in Section 5.1.1, counting algorithms (see Section 2.2.3.1.3 and Figure 9) were used to generate the temperature profiles of IGBT temperatures during operation. Using the cycle-counting algorithm of measured data, the total time spent ramping is not equal to the time spent dwelling at a constant temperature. The specific counting algorithm used was within the CALCE Simulation Assisted Reliability Assessment (CALCESARA) [94] Temperature Extraction Module. The time spent dwelling at the maximum and minimum cycle temperature is equal, as is the ramp rate in each part of the cycle. From the measured data of temperature cycling during normal operation presented in Figure 20a, the rainflow counting algorithm identified the cycling estimates presented in Figure 20b. The parameters for the cycle profiles estimated in Figure 20b are in Table 13.

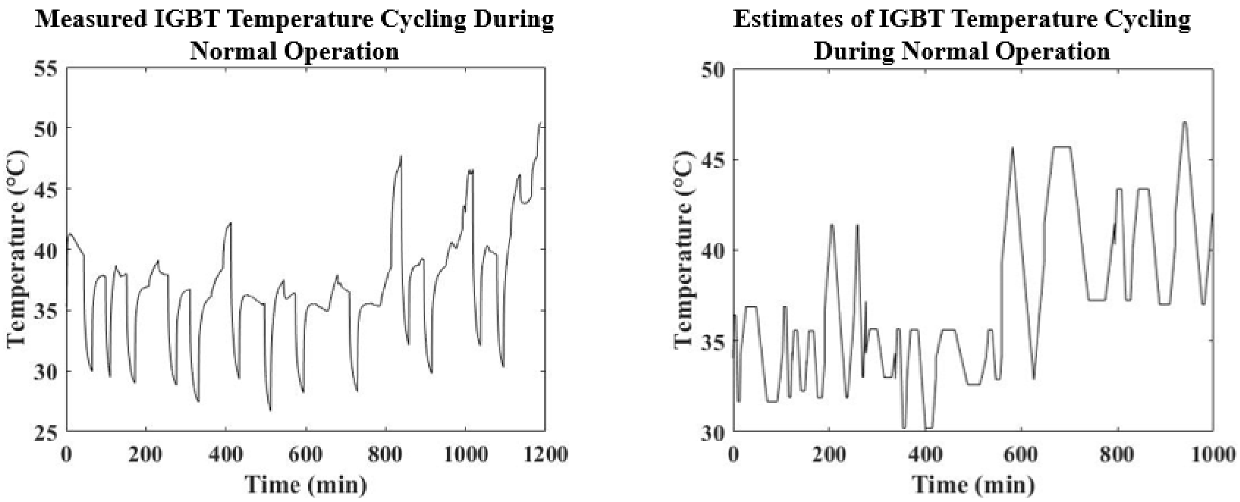

Figure 20: a) Measured IGBT temperature cycling during normal operation an. b) Estimates of temperature cycles during normal operation using the rainflow counting algorithm and the cycle profile in Figure 20.

Table 13: Parameters of temperature cycle estimates during normal operation, based on data presented in Figure 20b.

T_{min} (°C)	**T_{max} (°C)**	**T_{mean} (°C)**	**ΔT (°C)**	**Calculated Ramp Rate**	**$t_{D,max}$ and $t_{D,min}$**	**Duration**
32.66	36.41	34.535	3.75	93.75	24.92	50
31.68	36.41	34.045	4.73	126.13	7.59	15.33
31.68	36.9	34.29	5.22	122.82	43.75	87.67
31.92	36.9	34.41	4.98	132.80	9.34	18.83
32.25	35.61	33.93	3.36	79.06	15.29	30.75

31.89	35.58	33.735	3.69	86.82	18.25	36.67
31.89	41.39	36.64	9.5	0.75	5.59	62.00
33	41.39	37.195	8.39	2.01	3.50	23.67
33	35.67	34.335	2.67	71.20	30.34	60.83
30.21	35.67	32.94	5.46	128.47	12.00	24.17
30.21	35.64	32.925	5.43	135.75	29.92	60.00
32.59	35.63	34.11	3.04	71.53	52.00	104.17
32.89	35.63	34.26	2.74	68.50	16.17	32.50
32.89	45.69	39.29	12.8	0.59	0.75	88.33
37.24	45.69	41.465	8.45	5.34	70.00	146.33
37.24	43.37	40.305	6.13	153.25	18.92	38
37.02	43.37	40.195	6.35	158.75	43.92	88.00

In the case of temperature cycling during refrigerator pull-down (see Figure 21), however, the previously assumed cycling profile (Figure 10) is not fully representative of the temperature cycling occurring. Most cycling follows a different profile than before. Looking at the electrical loads (which are described in 5.1.2.2), the previously assumed cycling profile would not work, leading to the definition of the new cycling profile in Figure 22.

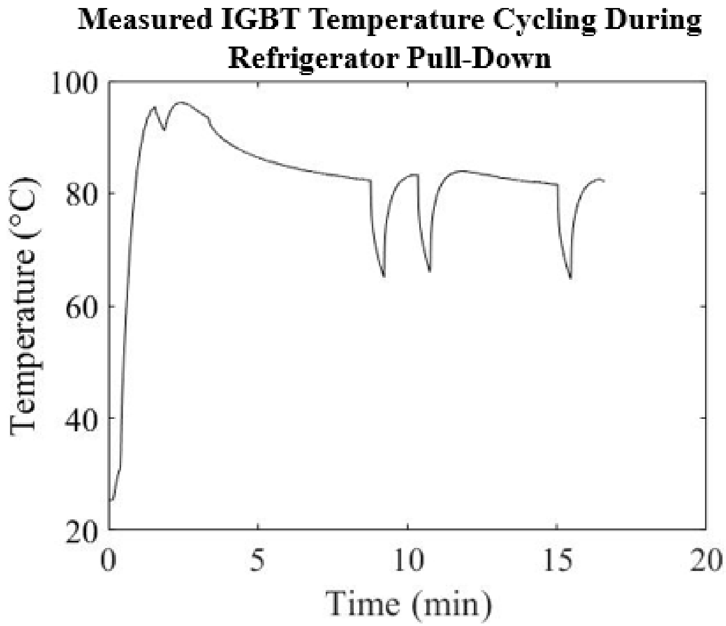

Figure 21: Temperature cycling measurements during refrigerator pull-down.

The newly defined cycling profile includes local minimum temperatures, as opposed to an assumed global minimum temperature, like in Figure 10. As a result, the cycle temperature range is the maximum value of the maximum cycle temperature minus each local minimum temperature. Additionally, there is no dwelling at either minimum cycle temperature, or all dwelling occurs at the maximum temperature. Because the profile assumes no dwelling at the minimum cycle temperatures, the previous profile was used for modeling temperature cycling during normal operation, as it had much more dwell time at the minimum temperature than the refrigerator pull-down does.

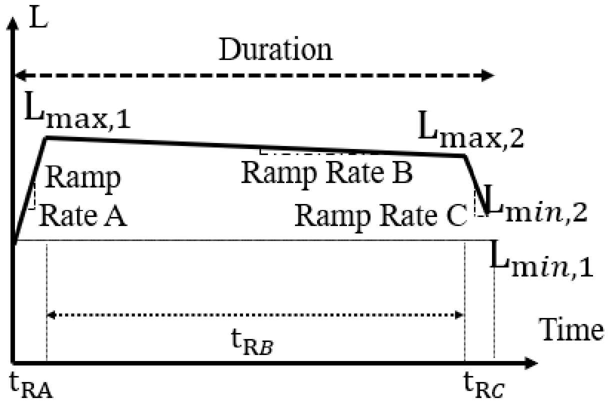

- L – variable for loading in cycle
- $L_{max,1}$ - first maximum temperature
- $L_{max,2}$ - ending maximum temperature
- $L_{min,1}$ - first minimum temperature
- $L_{min,2}$ - ending minimum temperature
- Duration – the total length of time of the cycle
- t_{RA}, t_{RB}, t_{RC} - time spent ramping at each ramp rate A, B, and C

$$Ramp\ Rate_A = \frac{L_{max,1} - L_{min}}{t_{RA}}$$

$$Ramp\ Rate_B = \frac{L_{max,2} - L_{max,1}}{t_{RB}}$$

$$Ramp\ Rate_C = \frac{L_{min} - L_{max,2}}{t_{RC}}$$

Figure 22: Alternative cycling profile used for modeling refrigerator pull-down temperature cycling, electrical loading, and normal operation electrical loading.

From the measured data in Figure 21 and the cycling profile in Figure 22, the corresponding estimated cycles for temperature cycling during refrigerator pull-down are in Table 14. Note that estimates of refrigerator pull-down temperature cycle and electrical loads and estimates of electrical loads during normal operation are optically derived, as opposed to using CALCESARA.

Table 14: Refrigerator pull-down temperature cycle parameter estimates.

$T_{min,1}$ (°C)	$T_{min,2}$ (°C)	$T_{max,1}$ (°C)	$T_{max,2}$ (°C)	Ramp Rate A (°C/min)	Ramp Rate B (°C/min)	Ramp Rate C (°C/min)	Duration (min)
20	65	95	85	50	1.70	50	8
65	65	85	85	50	0	50	3
65	65	85	85	50	0	50	5
65	85	85	85	50	0	50	1.5

5.1.2.2 Estimation of Electrical Loads in Refrigerator Operation

Estimating electrical loads during refrigerator operation will involve cycle-counting of electrical loads during refrigerator pull-down using measured data. However, normal operation electrical load estimation will use numerical estimates of electrical loads provided by the home appliances company and the cycling estimates from refrigerator pull-down. Measurements of the discrete IGBT collector-emitter current during refrigerator pull-down are in Figure 23.

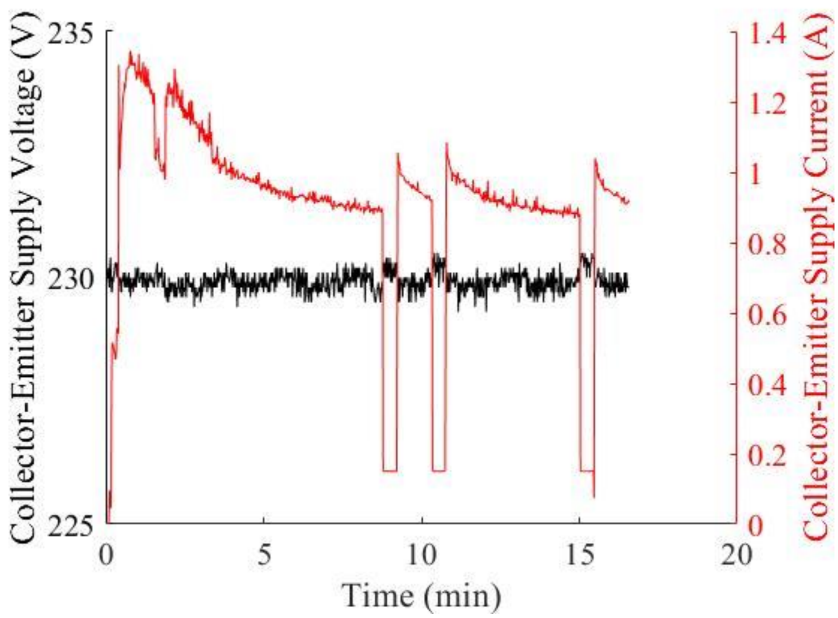

Figure 23: Measurements of discrete IGBT collector-emitter currents during refrigerator pull-down.

Based on the cycling profile demonstrated in Figure 22, Table 15 includes the estimates of electrical load cycling experienced by the discrete IGBT during the refrigerator pull-down procedure. The most common "Ramp Rate A" and "Ramp Rate B" (approximately 50 A/min and

-42 A/min, respectively) and the most common minimum collector-emitter current (0.2 A) apply to numerically estimate the loads experienced by the discrete IGBT during normal operation.

Table 15: Estimations of electrical load cycles experienced by the discrete IGBT during refrigerator pull-down.

$\mathbf{t_{RA}}$ (s)	$\mathbf{t_{R\mathit{B}}}$ (s)	$\mathbf{t_{R\mathit{C}}}$ (s)	$\mathbf{I_{m\mathit{in},1}}$ (A)	$\mathbf{I_{m\mathit{in},2}}$ (A)	$\mathbf{I_{max,1}}$ (A)	$\mathbf{I_{max,2}}$ (A)	**Ramp Rate A (A/s)**	**Ramp Rate B (A/s)**	**Ramp Rate C (A/s)**	**Duration (min)**
50	476	1	0.2	0.2	1.4	0.9	0.024	-0.001	-0.700	8
1	63	1	0.2	0.2	1.00	0.9	0.800	-0.002	-0.700	3
1	260	1	0.2	0.2	1.1	0.9	0.900	~ -8E-4	-0.700	5
1	60	1	0.2	0.2	1.04	0.92	0.840	-0.002	-0.720	5.5

Numerically estimating the electrical load cycles experienced during normal operation comes from the following details provided by the home appliances company: (1) The IGBT supply current is at most 0.6 A when the compressor is running. (2) The current can reach up to 2 A during start-up. Some additional assumptions are that: (1) Compressor start-up lasts 1 min at most. (2) Assume the approximate median normal operation cycle duration is 60 min; assume each current cycle is 58 min. (3) Assume turn-off takes approximately 1 min. (4) This process occurs 16 additional times in each period of operation to make 960 minutes of operation. (5) The remaining 40 minutes within the normal operation period is assumed to be idle time, with no applied electrical loads. This idle time is split into each normal operation cycle. Table 16 shows the resulting estimation of electrical load cycling during normal operation.

Table 16: Numerical estimates of electrical load cycling experienced by the discrete IGBT during normal operation.

t_{RA} (s)	t_{RB} (s)	t_{RC} (s)	$I_{min,1}$ (A)	$I_{min,2}$ (A)	$I_{max,1}$ (A)	$I_{max,2}$ (A)	Ramp Rate A (A / min)	Ramp Rate B (A/min)	Ramp Rate C (A/min)	Duration (min)
<1	59	<1	0.2	0.2	2	2	50	0	-42	1
<1	3400	<1	0.2	0.2	0.6	0.6	50	0	-42	58
<1	59	<1	0.2	0.2	0.6	0.6	50	0	-42	1
0	156	0	0	0	0	0	0	0	0	2.6

5.1.2.3 Collating Electrical and Thermal Loads Experienced During Operation

Figure 24 summarizes the timeline of loading that the discrete IGBT experiences during operation over its lifetime. Normal operation temperature cycling refers to the cycle estimates of temperature cycling data provided by the sponsor. Normal operation electrical loading refers to the numerical estimates of collector current experienced by the discrete IGBT during normal operation. As the duration of collected data for refrigerator pull-down temperature cycling and electrical loading is the same, no distinction is made between the two.

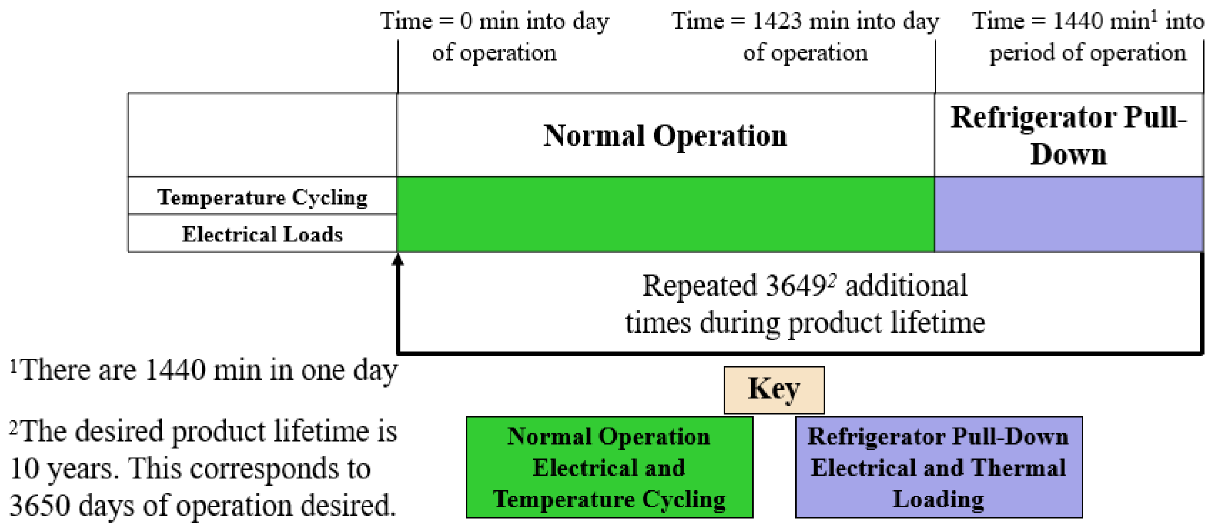

Figure 24: Timeline for loading experienced by the discrete IGBT during one period of operation repeated throughout the desired lifetime of 10 years.

5.2 Discrete IGBT Failure Mechanism Prioritization and Test Identification

Recall that before completing failure mechanism risk prioritization, one needs to identify potential failure mechanisms that can affect the product over its lifetime.

Table 17 includes examples of failure mechanisms that can affect the Infineon IKD06N60R discrete IGBT over its lifetime, with the corresponding failure modes, failure sites, and life cycle loads that contribute to the effects of the failure mechanisms. Based on the life cycle profile, most of the loading experienced by the product over its lifetime are electrical and temperature-related loads. Based on failure analysis conducted by the home appliances company, failures are attributed to elevated transient voltages and induced currents causing burning on both the gate area and the die surface. As a result, the dominant failure mechanisms for the IGBTs in this application could include die-attach delamination/voiding, latch-up, and gate oxide degradation. Based on the identified failure mechanisms and the cyclical nature of loading experienced by the product over its lifetime, the qualification tests most applicable for the discrete IGBT in the refrigerator motor inverter board are:

- High-Temperature Reverse Bias (HTRB)
- High-Temperature Gate Bias (HTGB)
- Intermittent Operating Life Test (IOL)
- Temperature Cycling Test (TC)
- High-Temperature Operating Life (HTOL)

Table 17: The failure modes, sites, and loading corresponding to discrete IGBT failure mechanisms.

Failure Mechanisms	Failure Modes	Life Cycle Loads	Failure Sites
Wirebond Cracking / Liftoff [95, 96]	Open circuit	High temperature, high current density	Wirebond
Die Attach Delamination / Voiding [95]	Open circuit	High temperature, high current density	Die attach
Latch-Up [95, 97]	Short circuit	High temperature, high current	Die

Failure Mechanisms	Failure Modes	Life Cycle Loads	Failure Sites
Gate Electrical Overstress [97, 98]	Open circuit	High temperature, high current density	Gate oxide
Avalanche Breakdown [96, 99]	Short circuit	Collector-Emitter Voltage Higher Than Rated Voltage	PN Junction
Hydrogen Proton Contamination (trench gate failure mechanism) [100, 101]	Open circuit	A variety of sources (e.g., moisture)	Gate oxide
Conductive Path Formation (trench gate failure mechanism) [101]	Short circuit	Moisture Accumulation	Boro-Phospho-Tetraethyl-Orthosilicate (BPTEOS) Surface of Trench Gate

5.3 Determination of IGBT Qualification Test Conditions and Durations

For the purpose of determining the required test conditions and durations to meet IGBT qualification requirements for this application, several IGBTs were tested until failure was observed. In this case, failure corresponds to the first instance of latch-up in testing, where the collector current would increase uncontrollably above the normal operating collector current. The test itself was an intermittent operating life (IOL) test with an elevated operating temperature, where the parameters required for test development are in Table 18. As a result, this is also a high-temperature operating life test. A sample data set is studied and discussed in more detail in Section 5.4.

Table 18: Test parameters for the discrete IGBT intermittent operating life test.

Intermittent Operating Life Conditions							
On-Time (s)	Off-Time (s)	$V_{CE,max}$ (V)	$\frac{dI_C}{dt}$ (A/s)	$\frac{dV_{GE}}{dt}$ (V/s)	Operating Temperature (°C)	Sampling Frequency (Hz)	Number of Samples
30	30	10	3	1.5	150	20	6
70	90	10	3	1.5	150	20	6
90	60	10	3	1.5	150	20	6

The authors cannot reveal observed times-to-failure from testing. However, based on the tests involving elevated operating temperatures and bias conditions, assume the Boyko and Gerlach-Modified Generalized Two Stress Eyring Model (Temperature-Voltage Acceleration Model) [41, 42]. For more information regarding the model, refer to Table 19. In order to solve for the model constants, applying the natural log function linearized the equation, and the updated linearization is also in Table 19.

Table 19: Boyko and Gerlach-Modified Two Stress Eyring Model revisited.

Time-To-Failure Model	**Equation for Estimating Time-to-Failure**	**Variables in Equation**
Boyko and Gerlach-Modified Generalized Two Stress Eyring Model (Temperature-Voltage Acceleration Model) [41, 42]	$\mathrm{TTF} = \gamma_{0} * e^{\frac{-E_a}{k} * \left(\frac{1}{T_{max,test}}\right)} * e^{\gamma_{1} * ln\left(V_{max,test}\right) + \gamma_{2} * \frac{ln\left(V_{max,test}\right)}{k * T_{max,test}}}$	TTF ~ Time-to-Failure T, V ~ temperature and voltage, respectively max, use ~ maximum value of each loading cycle in lifetime max,test ~ maximum value of each loading cycle used for testing E_a ~ activation energy k~ Boltzmann constant ($= 1.381 * 10^{-23}\ \frac{J}{K}$) γ_{12}, γ_{3} ~ model constants Note that for model solve simplification, $\gamma_{12} = \gamma_{1} - \gamma_{2}$
Time-To-Failure Model	**Equation for Estimating Time-to-Failure**	
Linearized Boyko and Gerlach-Modified Generalized Two Stress Eyring Model	$ln(TTF) = \boldsymbol{ln(\gamma_0)} * \left(\frac{E_a}{k * T_{max}}\right) + \boldsymbol{\gamma_2} * ln(V_{max}) + \boldsymbol{\gamma_3} * \left(\frac{ln(V_{max})}{k * T_{max}}\right)$ **(Model constants to solve are emboldened)**	

With the model constants now known, calculate each acceleration factor corresponding to the different operation cycles using the following equation. The acceleration factor model version of the Boyko-Gerlach Modified Generalized Two Stress Eyring Model is in Table 6. In order to calculate the required number of cycles to meet the qualification requirements, one could use the below equation. The acceleration factor equation seeks to determine the required number of cycles of testing that would meet the requirements of the product. Each cycle within the product lifetime would correspond to an equivalent amount of testing time given a known testing profile, and summing the equivalent testing time for all product lifetime cycles would result in the total required testing to meet the product lifetime requirements.

$$\mathrm{N_{qual}} = \sum_{\mathrm{i=1}}^{\mathrm{C}} \frac{1}{\mathrm{AF_i}}$$

where:

- $\mathrm{N_{qual}}$ - required number of qualification cycles
- C – total number of cycles in product lifetime
- $\mathrm{i} \in \mathrm{C}$ – indexing through each cycle in the order of occurrence
- $\mathrm{AF_i} = \frac{N_{use}}{N_{test}}$ - acceleration factor for each cycle in the order of occurrence.

5.4 Applying Diagnostics and Prognostics Techniques to IGBT Qualification

For the purpose of demonstrating the application of diagnostics and prognostics techniques, the author generated some synthesized test data. As a result, any results observed from test data and discussed times-to-failure or anomalous behavior should not be considered representative of behavior observed for this IGBT or any IGBT. Instead, the methods demonstrated are the focus, and the assumption is that these methodologies apply in other contexts. The precursor parameter trends that were synthesized were: collector current, gate current, collector-emitter voltage, and gate-emitter voltage. The trends are all in Figure 25.

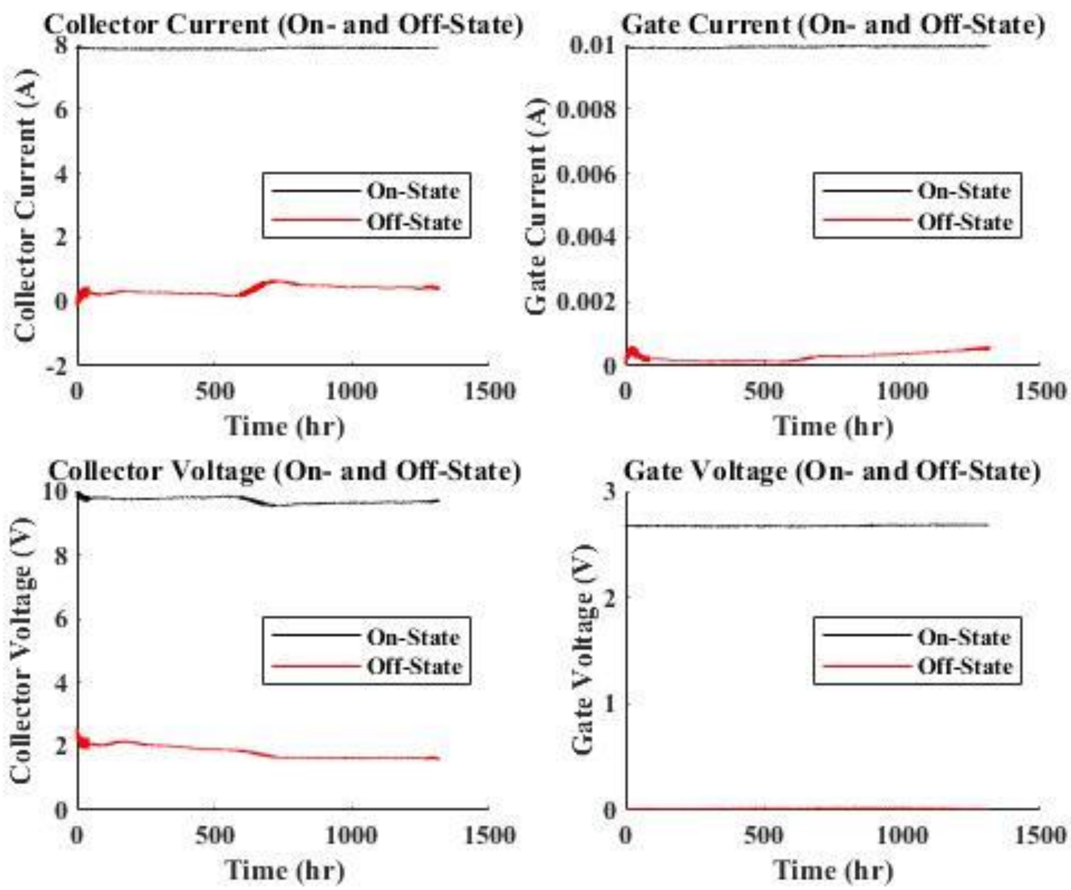

Figure 25: Collector current, gate current, collector-emitter voltage, and gate-emitter voltage measurements over testing. Note that the collector voltage and gate voltage refers to the "collector-emitter" voltage and "gate-emitter" voltage.

The synthesized data is based on data measured by NASA's Ames Research Center's Prognostics Center of Excellence. The IGBTs under test are Infineon IGBT Part Number IRFG4BC30KD. The test conducted by the Ames Research Center included that the collector-emitter voltage was held at 10 V until the case temperature reached 270°C, after which the IGBT was turned off. Testing occurred for four hours at a measurement rate of 20 Hz. Failure under testing occurred due to a latch-up event where thermal runaway with temperatures exceeding 305°C occurred.

The synthesized data used in this example is derived from the Ames Research Center data by first preserving the trends by assuming an N-degree polynomial fit. Depending on the trend, N was between 10 and 15. The timeline for testing was extended from around 4 hours to over 1300 hours to represent a longer test under less accelerated test conditions. Additionally, to imitate the noise that was present in the original data, some noise was introduced to the synthesized data, with a standard deviation (stdev) calculated every 40 hours and between rand(-2,2)*stdev added to each measurement to simulate noise that would be observed over testing.

5.4.1 Anomaly Detection Using Mahalanobis Distance

These measurements are then used for anomaly detection. In this example, the Mahalanobis distance approach to anomaly detection classifies the datapoints as being within acceptable parameters or abnormal. Using the first 150 hours of measurement as representative of normal behavior, abnormal measurements are measurements beyond three standard deviations (3σ) of the representative sample from the mean of the representative sample (μ). This corresponds to Nelson's First Rule for out-of-control variable detection [102], which also corresponds to the approach taken by Patil et al. [70].

5.4.1.1 Introduction to Mahalanobis Distance and Application to Measured Parameters

Originally introduced in 1936 by P.C. Mahalanobis [103], Mahalanobis distance is an approach for calculating the distance between a single point and a data distribution. Unlike Euclidean estimations of distance, Mahalanobis distance accounts for correlations within the dataset to calculate a unitless, scale-invariant "distance" between the single point and data distribution. The equation for Mahalanobis distance (MD) is as follows:

$$MD(X_i) = \sqrt{(X_i - \mu)^T S^{-1} (X_i - \mu)}$$

where:

- X_i is the measured data.
- μ is the mean of the reference data set.
- T is the transpose operator.
- S is the covariance matrix.

As previously mentioned, the anomalous boundary to be utilized is $\mu+3\sigma$, where values of the test data that go beyond 3σ from the μ of the reference dataset are considered abnormal. Note that the exact value of $\mu+3\sigma$ is transformed into the Mahalanobis space by solving $MD(\mu+3\sigma)$. Additionally, the data is normalized by dividing each value by the mean of the healthy dataset for the given trend. Applying the Mahalanobis distance approach to all eight electrical measurements of IGBT behavior, Figure 26, Figure 27, Figure 28, and Figure 29 include the results.

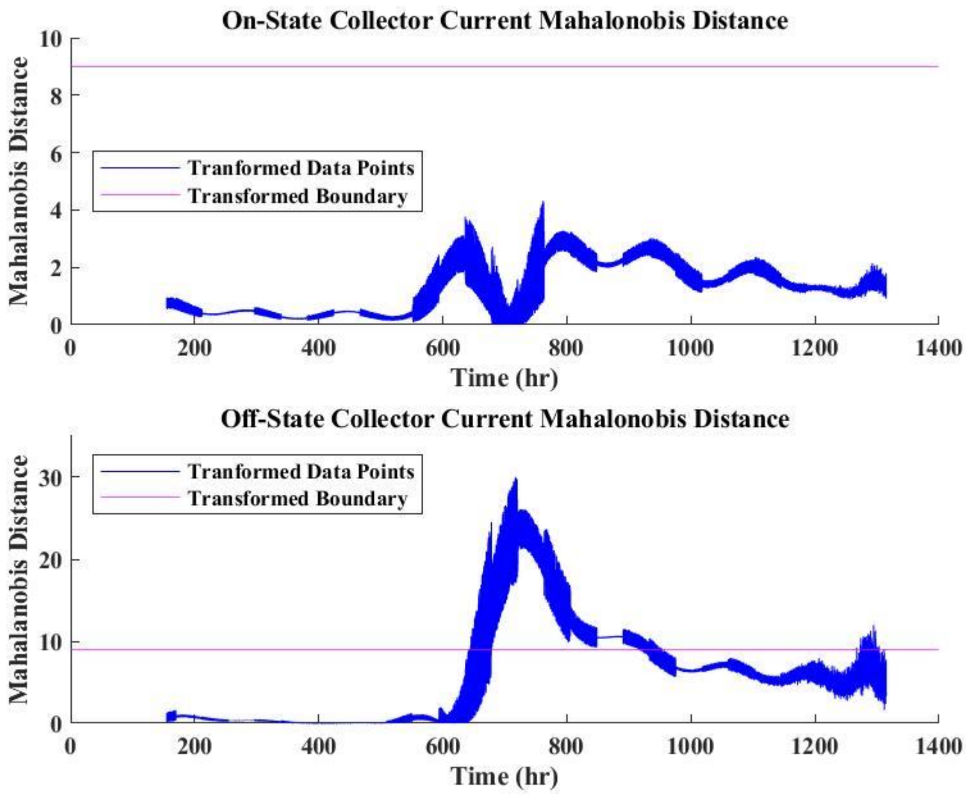

Figure 26: Mahalanobis distance-transformed measurements of collector current in both on and off states.

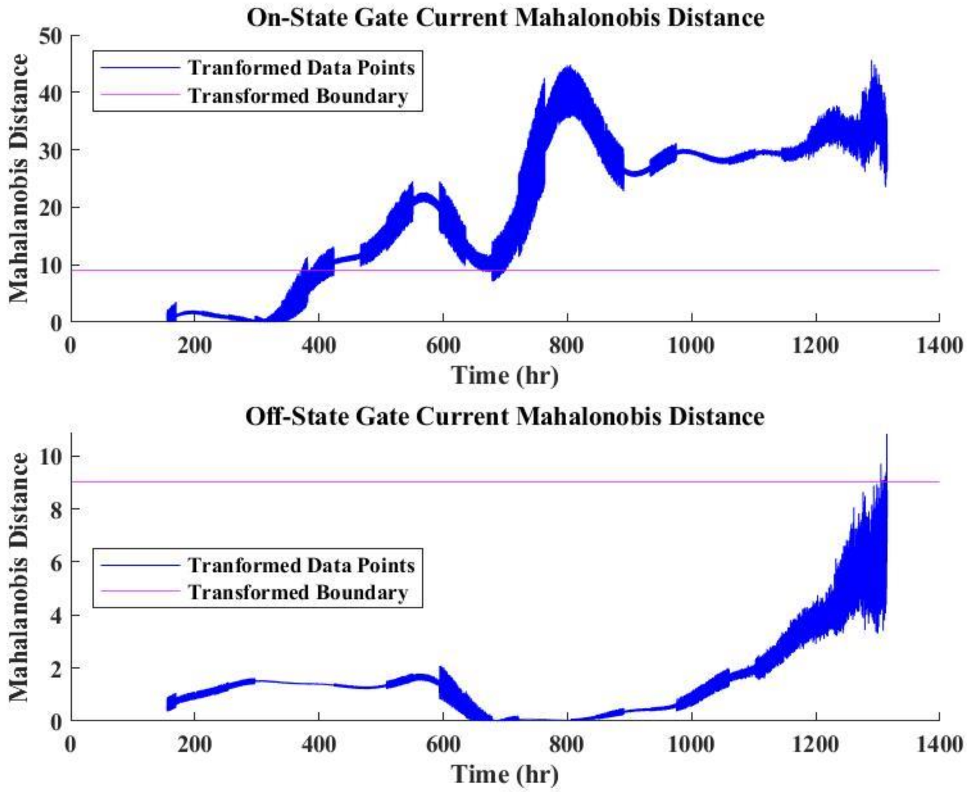

Figure 27: Mahalanobis distance-transformed measurements of gate current in both on and off states.

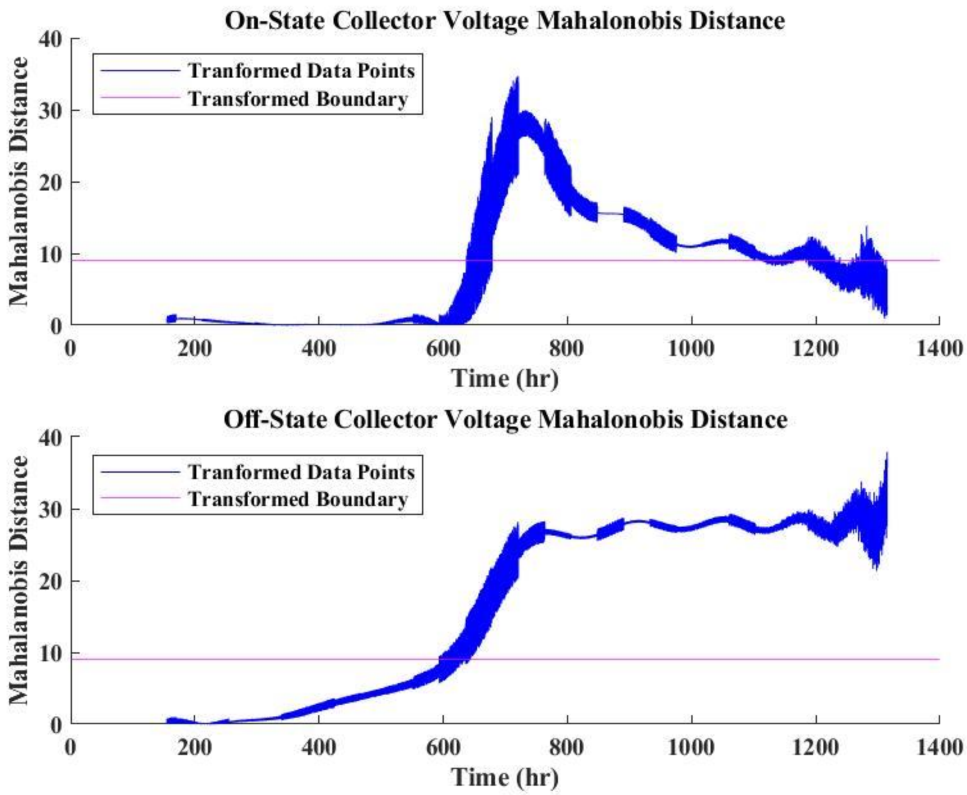

Figure 28: Mahalanobis distance-transformed measurements of collector-emitter voltage in both on and off states.

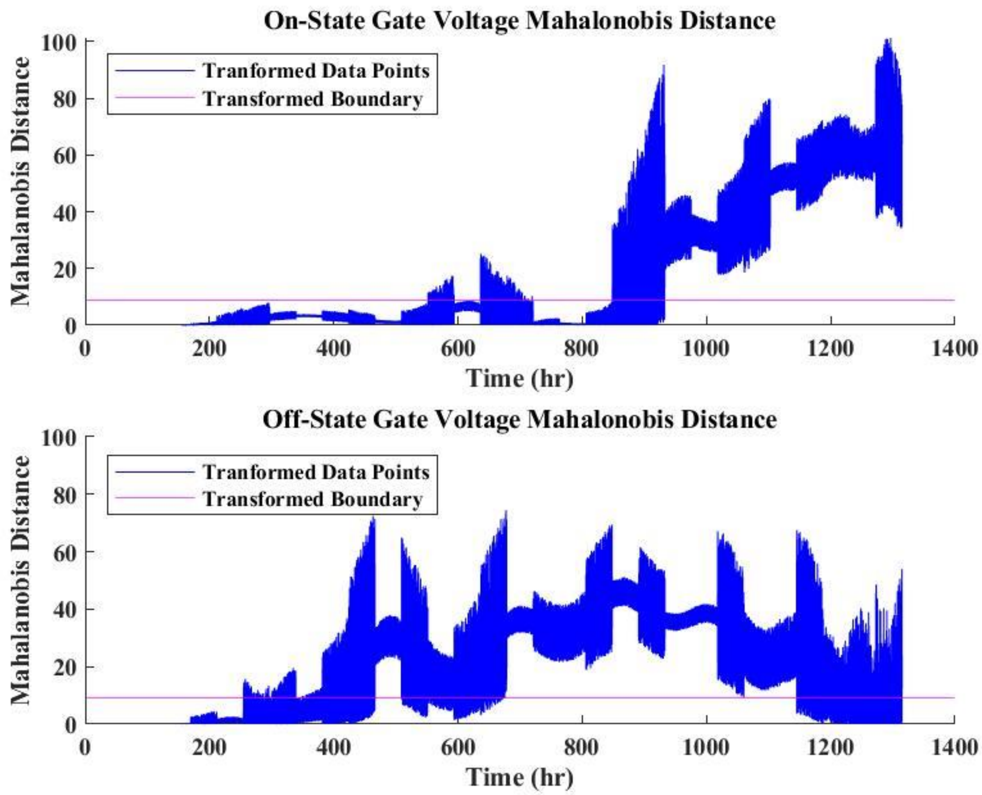

Figure 29: Mahalanobis distance-transformed measurements of gate-emitter voltage in both on and off states.

After studying each parameter trend after being Mahalanobis-transformed, several parameters presented anomalous behavior far before failure at 1300 hours. The off-state collector current revealed anomalous behavior at approximately 600-650 hours of testing, as did the on-state collector-emitter voltage, off-state collector-emitter voltage, and the on-state gate-emitter voltage. The on-state gate current demonstrated anomalous behavior 400 hours into testing. The off-state gate voltage observed anomalous behavior as early as 250 hours into testing. The on-state collector current and off-state gate current did not present evidence of anomalous behavior throughout the test, and the off-state gate current showed anomalous behavior only towards the end of testing when the failure occurred. Towards the end of testing, the off-state collector current, on-state collector-emitter voltage, and off-state gate voltage measurements became less anomalous and began to approach the anomalous boundary. The off-state collector-emitter voltage and on-state gate current showed steady anomalous behavior after 600 hours, and the on-state gate-emitter voltage showed steady anomalous behavior after 900 hours.

5.4.1.2 Application of Mahalanobis Distance to Calculated Parameters

The on-state gate resistance (electrical), on-state collector resistance (electrical), and transconductance are analyzed during testing using the data provided. The equations for solving each of these parameters are in Table 20. These are examples of precursor parameters that can come from other precursor parameters and better highlight certain types of product behavior than the individual parameters would. The parameters before the Mahalanobis transformations are in Figure 30. Note that the unit for transconductance is Siemens, which is analogous to the inverse of resistance.

Table 20: Equations for calculating on-state collector resistance, on-state gate resistance, and transconductance.

Precursor Parameter	**Calculating Each Precursor Parameter**
On-State Collector Resistance ($R_{On,C}$)	$R_{On,C} = \frac{\mathrm{V}_{\mathrm{CE},on}}{I_C}$
On-State Gate Resistance ($R_{On,G}$)	$R_{On,G} = \frac{\mathrm{V}_{\mathrm{GE},on}}{I_G}$
Transconductance (g_m)	$g_m = \frac{I_C}{V_G}$

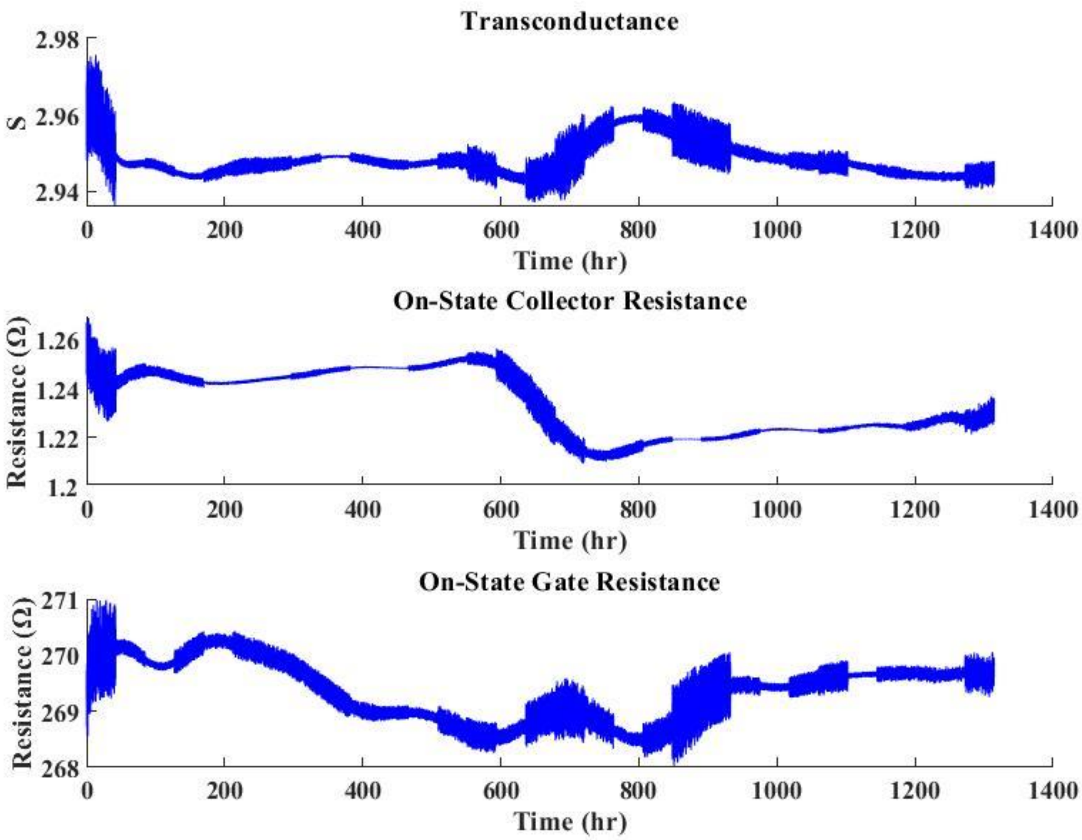

Figure 30: Transconductance, on-state collector and on-state gate resistance as calculated from the previously measured precursor parameters.

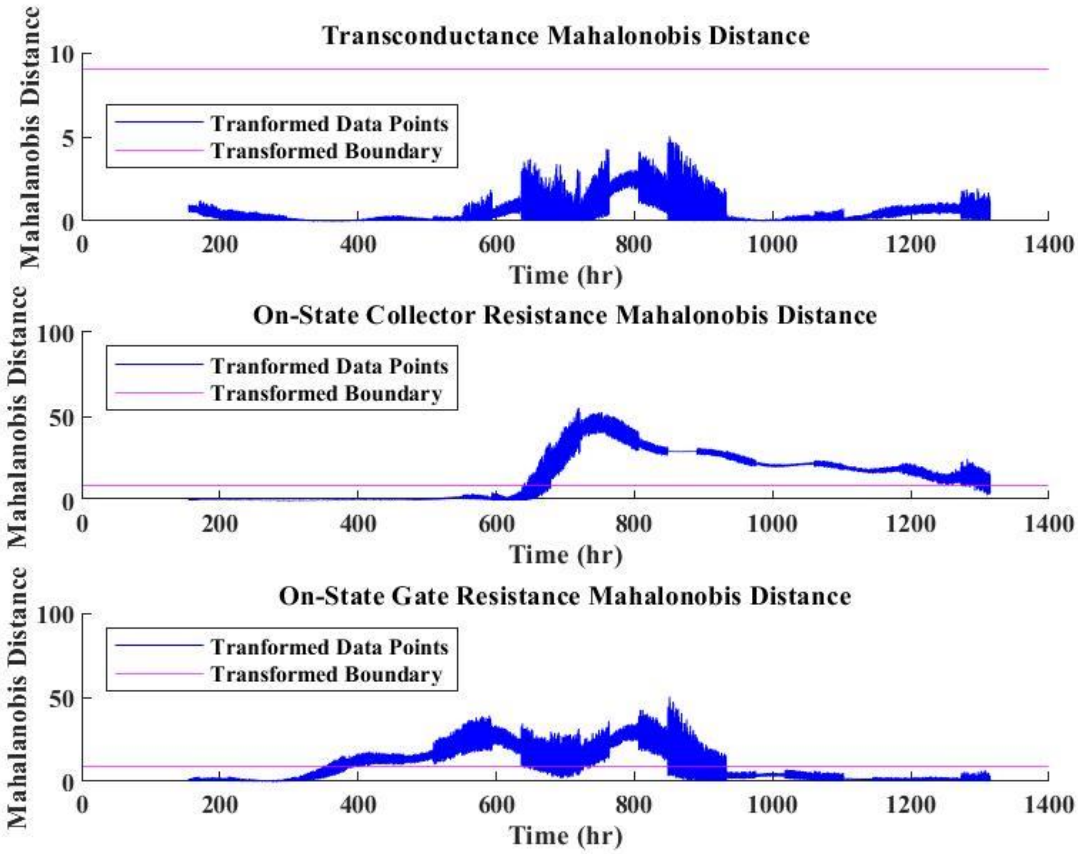

Figure 31: The Mahalanobis transformations of the transconductance, on-state collector, and on-state gate resistance.

Figure 31 includes the results from the Mahalanobis transformations. The Mahalanobis-transformed transconductance of the discrete IGBT over testing does not reveal any anomalous behavior. The transformed on-state collector resistance reveals anomalous behavior at around 650 hours (around the same time as the off-state collector current, on-state collector-emitter voltage, off-state collector-emitter voltage, and on-state gate-emitter voltage.) Over the testing period, the transformed trend returns toward the anomalous boundary. The transformed on-state gate resistance first presents anomalous behavior at approximately 400 hours, but after about 900 hours, the behavior returns below the anomalous boundary.

5.4.1.3 Mahalanobis Distance Using Combinations of Parameter Measurements

Recall that Mahalanobis distance is a unitless, scale-invariant distance between a data point and a data distribution. This also allows calculating this distance between an N-dimensional point and a corresponding data distribution. As a result, three different combinations of parameter measurements went through Mahalanobis-distance-based anomaly detection at each point in time. The on-state gate current, off-state gate voltage, and on-state gate resistance all experienced anomalous behavior at 250 or 400 hours. The combination of these parameters will be referred to as Anom400. The off-state collector current, on-state collector-emitter voltage, and on-state collector resistance demonstrated anomalous behavior at 650 hours and will be denoted as Anom650. The set of all anomalous parameters is made of the total 9 trends that demonstrated anomalous behavior and will be called AnomAll. Figure 32 includes the Mahalanobis transformation of Anom400, Anom650, and AnomAll.

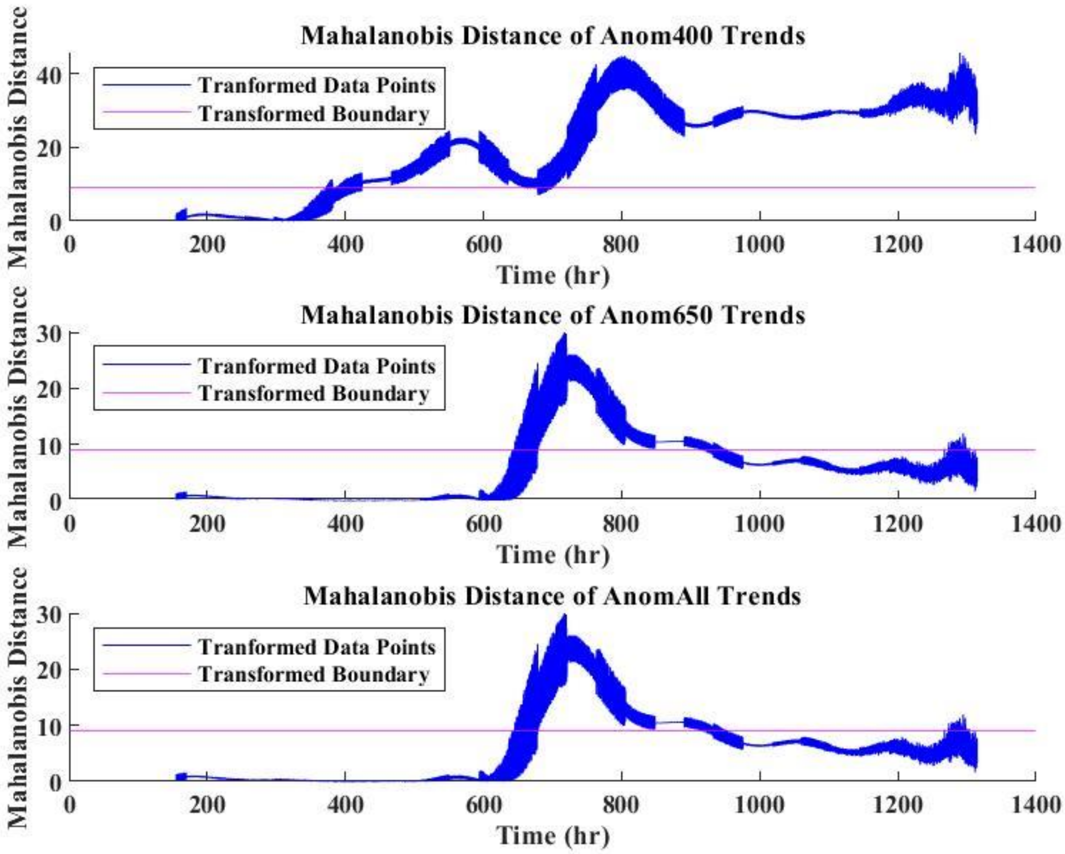

Figure 32: The Mahalanobis transformations of Anom400, Anom650, and AnomAll.

Anom400 showed anomalous behavior at 400 hours and almost healthy behavior at 650 hours before continuing to be anomalous. Anom650 showed anomalous behavior at 650 hours and healthy behavior after about 950 hours. After 950 hours, Anom650 showed healthy behavior for the remainder of the test. AnomAll appeared to have been biased heavily by the parameters making up Anom650, as both Anom650 and AnomAll demonstrate extremely similar results. In previous studies, many authors used combinations of parameter trends for anomaly detection, and the above trends highlight that a tailored and careful selection of parameters is crucial for anomaly detection.

Simply combining all anomalous parameters would have hidden the fact that anomalous behavior could have been predicted much earlier and throughout the remainder of the test.

One can combine parameters in multiple ways for anomaly detection. As demonstrated, one approach for combining parameters is to combine based on when anomalous behavior was first detected. Another example is to combine parameters based on the failure effects observed. If failure analysis revealed multiple types of failure effects occurring, combining parameters based on the corresponding failure effects could apply to studying the timeline for different types of anomalies to manifest. An additional example is to combine parameters based on the types of anomalous behavior observed over the test. For instance, if multiple parameters demonstrated healthy behavior simultaneously after previously demonstrating anomalous behavior, this could point to instances where the component has recovered in some capacity.

5.4.1.4 Using Anomaly Detection for Data-Drive Failure Mechanism Identification

Refer to the list of precursor parameters and corresponding failure mechanisms included in Table 8 and knowledge of IGBT performance behavior. The increased on-state gate-emitter voltage would correspond to an increased gate threshold voltage required for IGBT turn-on, corresponding to gate oxide degradation (Table 8). Increased gate current also implies a larger power draw needed to operate the IGBT, which could be attributed to accumulating damage to the gate over the testing period. Using knowledge gathered from the study of IGBT modules, the anomalous on-state resistance for both collector and gate regions points to the degradation of both regions. Additionally, the anomalies present in the off-state collector current, on-state collector-emitter voltage, off-state collector-emitter voltage, and on-state gate current could also point to wirebond-related failure mechanisms, such as bond-wire liftoff and bond-wire fatigue.

Using the Mahalanobis distance-based anomaly detection technique on multiple IGBT precursor parameter trends, anomalous behavior appeared at least 700 hours before failure occurred. Using the off-state gate voltage trend, anomalous behavior occurred over 1000 hours before failure. However, other benefits arise from using anomaly detection during qualification or other types of testing.

Knowing how different failure mechanisms can impact precursor parameter measurements, one can identify other possible failure mechanisms that contribute to failure in the application environment. This allows for further reprioritization of failure mechanisms and can contribute to an improved understanding of the testing requirements needed for the product in that application. In this example, though gate-related failure signatures were observed during failure analysis, the data-driven failure mechanism identification approach reveals that some wirebond-related failures also occur.

5.4.1.5 Additional Benefits from Anomaly Detection

Conducting anomaly detection during qualification can provide information about component behavior under loading without being limited to data gathered during operation. Knowing more about component behavior while still under testing can supports efforts related to component selection, where one may consider different components for use in the intended application. Applying anomaly detection techniques provides the opportunity to determine when anomaly detection would be detected and also the types of anomalous behavior detected. Consider in the anomaly detection examples in Sections 5.4.1.1-5.4.1.3 that different parameters not only demonstrated anomalous behavior at different times, but also periods where the parameters would exhibit healthy behavior, intermittently healthy and anomalous behavior, periods of increasing/decreasing anomalous behavior, and other types of behavior. These types of comparisons (time-to-anomalous-behavior, anomalous parameter behavior) can be comparisons to make between different types of components that one can use in this application.

Other examples of benefits that arise from applying anomaly detection techniques to qualification or other types of testing apply to prognostics and health management systems in the application environment. For instance, one can validate different techniques for anomaly detection well before the product is placed in the application, therefore aiding in the development of monitoring systems. Additionally, trends observed during testing under different stress conditions can particularly contribute to condition monitoring.

5.4.2 Remaining Useful Life Estimation Using a Particle Filter

Recall from Section 4.3 that the particle filter calculates the remaining time-to-failure by first estimating the Bayesian posterior distribution of possible times-to-failure. Estimates of prior distributions influence the weights associated with the "particles," which then influence the posterior distribution estimate. Using the data measured during testing after the first appearance of anomalous behavior (approximately 250 hours), the authors continuously applied a particle filter to estimate the remaining-time-to-failure. Ultimately, the goal is to yield an accurate result as soon as possible to demonstrate that failure would occur either before or after the completion of the qualification test.

Using MATLAB's particle filter workflow [104] and *stateEstimatorPF* object, the authors ran different trends through the particle filter state estimator. Each particle filter iteration used 10,000 particles and a covariance matrix of 0.01*I(3), where I(3) corresponds to a 3x3 identity matrix. From the time of first anomaly detection (approximately 250 hours, based on the off-state gate voltage trend), the particle filter estimated the measurements at the next time step, with the measurements corrected only for an additional 250 hours (up to 500 hours into testing.) After that point, the particle filter object only made estimations with no corrections via measured data.

A study of different trends revealed that the off-state collector current, off-state collector-emitter voltage, and on-state gate resistance were best modeled by the particle filter approach. Figure 33 includes graphical representations of the results from the particle filter. The results show that with only the first 750 hours of data after anomalous behavior was first observed, the particle filter could forecast the future trends for the off-state collector current, off-state collector-emitter voltage, and the on-state gate resistance. This implies that one may be able to estimate the remaining-time-to-failure for the product well before the failure occurs, with more knowledge of how different trends are correlated with each other and how different types of failures present themselves. Being able to estimate remaining-time-to-failure for the product even after the qualification test is over can support parts selection and management. Consider a situation where one is using qualification to choose between multiple IGBTs for an application. In that instance, estimating time-to-failure aids in developing a time-to-failure distribution for the IGBTs under the test conditions. The time-to-failure distribution can act as another parameter to influence the IGBT selection to use in that application.

By analyzing additional test data, one can develop an approach for health monitoring using the results from these particle filter trends. This approach for health monitoring would be applicable for monitoring the product during testing and operation. The estimation of remaining-time-to-failure can be recalculated as a remaining useful life in operation by applying the same acceleration factor principles described in Section 5.3.

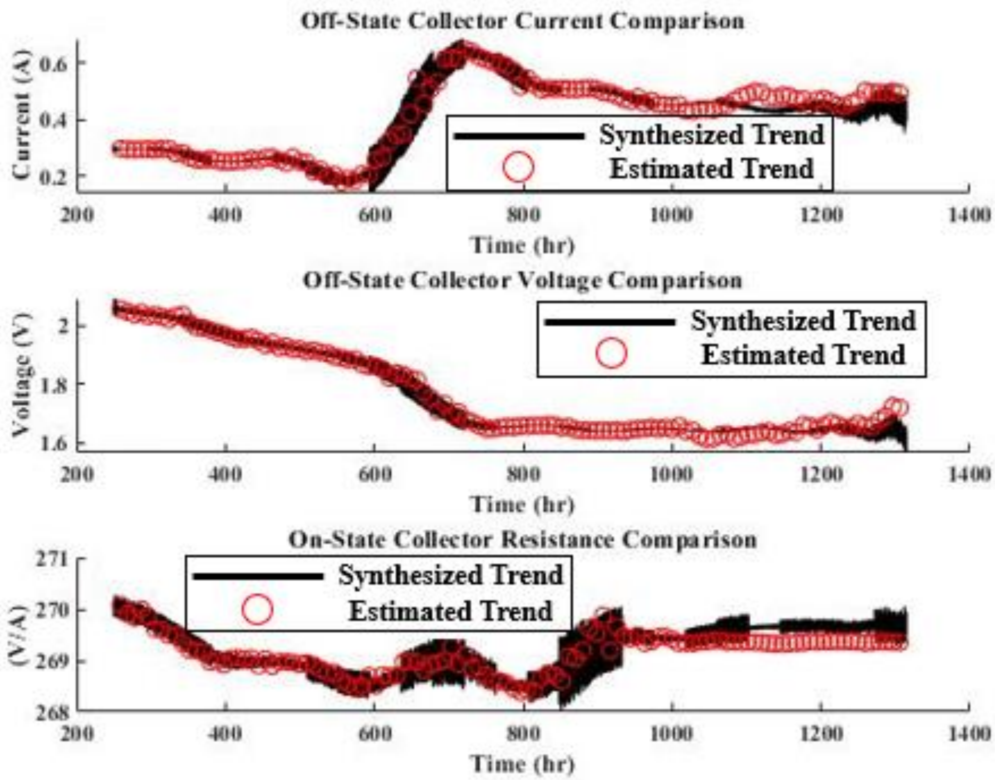

Figure 33: Particle filter results using the off-state collector current, off-state collector-emitter voltage, and on-state resistance.

Calculating the remaining useful life via the remaining-time-failure involves solving equations (shown below.) The first equation compares the time completed in testing to the equivalent amount of product lifetime that has occurred. The goal for the first equation is to solve for *G*, which is the equivalent amount of product lifetime cycles that have occurred during testing so far. The second equation uses knowledge of the remaining-time-to-failure in testing to calculate *D*, which is the equivalent number of cycles into product operation at which product failure is estimated to occur. With a theoretical estimate of time-to-failure in the product lifetime, one can estimate the remaining useful life for the product in operation. Knowing the remaining useful life, one can develop an initial maintenance and spare delivery schedule before the product is introduced into the application environment.

$$k * N_{qual} = \sum_{i=1}^{G} \frac{1}{AF_i}$$

$$RTF \cong \sum_{i=G}^{D} \frac{1}{AF_i * f_i}$$

where:

- RTF ~ remaining time to failure in qualification
- k ~ fraction of qualification test completed
- f ~ frequency of each cycle
- N_{qual} ~ required number of cycles for qualification
- G ~ equivalent cycles that already occurred during qualification testing
- D ~ equivalent cycles for time to failure in operation
- C ~ total number of ordered cycles
- $i \in C$ ~ indexing through each ordered cycle.
- AF_i ~ acceleration factor for each ordered cycle

6 Summary of Approach, Contributions, and Future Work

Product qualification, as an IEEE 1624 reliability program activity, intends to evaluate that products can meet the requirements for operation set forth by the intended application and the application environment. These requirements of operation, as defined by IEEE 1332, are product functionality, duration, life cycle conditions, and desired reliability metrics. Further study of published qualification standards from various organizations revealed that none of these standards included approaches for accounting for customer requirements and product physics-of-failure. A survey of 62 organizations conducted by Grosskopf et al. [9] revealed that 70% of those organizations refer to qualification standards. Within that 70%, 36% of those organizations use the qualification recommendations included in the standards even though the recommendations do not meet the organizations' requirements. 61% of all respondents also saw the need for better aligning qualification practices with intended application requirements.

6.1 Summary of Recommended Approach

This thesis focused on addressing these pitfalls in product qualification, particularly from the perspective of an electronic product manufacturer who is trying to assess if a component or subsystem within the product would meet intended application requirements. The application-specific procedure that arose from these efforts involves using the life cycle profile for the component/subsystem from the end of manufacturing through to its end of life and the application of failure modes, mechanisms, and effects analysis to determine the failure mechanisms that should be prioritized for the product in this application. Using the prioritized failure mechanisms, one can identify the required tests to ensure that the product can meet the intended application requirements. Using the life cycle profile, acceleration factor models, and published test method standards, one can determine the qualification test condition profile, the corresponding duration of testing, and industry-accepted approaches for conducting the qualification test. Following this, diagnostics and prognostics techniques are applied to tests within the procedure to hasten the qualification procedure potentially and to study product behavior under testing. Precursor parameters that one can use to track product behavior over testing arise from knowledge of the prioritized failure mechanisms, historical test data, and published research from similar technologies.

The life cycle profile for the product should consider how different geographical locations, climates, times of the year, manufacturing facilities, intended applications, and other factors can vary between one set of components and another. By accounting for life cycle phases (and differences therein), one can identify the most representative or even the most severe life cycle profile. Additionally, the life cycle profile should account for loads experienced by the component/subsystem during operation while being assembled into the electronic product and during storage/transportation, providing a more accurate profile of the loads that the component would experience throughout its lifetime. An accurate profile of the loads goes towards better failure mechanism prioritization and more accurate calculation of qualification conditions and duration requirements.

To mitigate the financial impact associated with qualification testing, a study of testing conducted on similar products can reveal that conducting certain tests would be redundant. Additionally, the application of diagnostics and prognostics techniques to product qualification can reveal anomalous product behavior and an estimation of when failure would occur well before the failure occurs - knowing that the product is demonstrating anomalous behavior and being able to predict when failure will occur means that one can stop testing early, thereby reducing the time required to complete product qualification.

6.2 Thesis Contributions

This thesis' first contribution is the synthesis of the life cycle profile before and during operation, failure prioritization, and diagnostics and prognostics techniques to develop an application-specific qualification procedure. Supplementing this application-specific approach for qualification procedure development is an example of using a component in a real-world application to demonstrate the whole process. With modifications, this application-specific approach could apply to other examples of conducting qualification. For instance, in the case of the qualification of individual components by an original component manufacturer, the application requirements could be set by industry best practices or by a particular qualification standard. In that instance, one can still implement prognostics and diagnostics techniques to better understand product behavior under different types of loading.

The second set of contributions of this thesis includes methods for discretizing the life cycle profile to better study loading throughout, providing examples of loads that can be qualitatively categorized for load quantification, and examples of variations in the life cycle profile that can occur before operation begins. The procedure in this thesis is a synthesis of the second set of contributions and ideas presented in several different publications and guides pertaining to life cycle profile development (e.g., considering loading before operation, variations in loading that can occur during operation, the types of loading that can occur, and methods for characterizing loading.)

The third contribution of this thesis is guidance on using diagnostics and prognostics techniques applied to qualification data to develop an improved qualification procedure, support component selection efforts, and evaluate the application of these techniques to condition monitoring and prognostics and health management efforts in operation. Pecht et al. [48, 49] discussed how prognostics-based qualification could reduce the time and resources required to conduct qualification and how one can reprioritize failure mechanisms. This thesis analyzed how to use diagnostics and prognostics techniques for component selection and improving the qualification procedure. In this thesis, qualification procedure improvement is better targeting the procedure towards the application requirements, as opposed to reducing the time and resources required to conduct qualification. The assumption is that each test needs to be fully conducted or previously had been conducted in order to qualify the product. Data-driven anomaly detection can be used to reprioritize failure mechanisms for the component in the intended application, which can apply to improving the qualification procedure to make it more targeted to application requirements. The times-to-anomalous behavior, types of anomalous behavior observed, and estimated times to failure under qualification loading conditions can be points of comparison used for component selection for the intended application. Finally, the application of data-driven diagnostics techniques and prognostics to data representative of product behavior under loading can be used to test the potential effectiveness of these techniques during electronic product operation.

6.3 Examples of Future Work

The scope of this thesis was limited to developing a qualification procedure for a single component or subsystem within an electronic product. In reality, qualification can occur at any stage in the product life cycle, be it for a single component, an electronic assembly (e.g., the refrigerator motor inverter board), as part of an integrated product (e.g., the refrigerator), or at other levels. Future studies of application-specific approaches for developing qualification procedures could look at qualification at these or other levels and how the approach would correspondingly change.

Additionally, the focus of this thesis was primarily related to discrete insulated gate bipolar transistors, with some discussion on insulated gate bipolar transistor modules. There have been a wide variety of studies of the application of prognostics and diagnostics to the behavior observed in other electronic components and products (e.g., capacitors, LEDs, batteries), and the promising results from these studies reveal that one could also apply prognostics and diagnostics techniques to product qualification for these components. Another example of future work would be to study further the ancillary benefits of applying prognostics and diagnostics to product qualification. Although a couple of examples were highlighted in this thesis, more data would better demonstrate the ideas presented and may open new avenues of study. Some examples of new avenues could include studying how different parameter trends correlate with each other and how to develop product sustainment practices that can be applied to products during operation during the qualification stage.

7 Bibliography

[1] K. C. Kapur and M. Pecht, Reliability Engineering, A. P. Sage, Ed., Hoboken, NJ, USA: John Wiley & Sons, Inc., 2014, pp. 147-168.

[2] *IEEE 1624: Standard for Organizational Reliability Capability,* New York City, NY: Institute of Electrical and Electronics Engineers (IEEE), 2008.

[3] *IEEE 1332: Standard Reliability Program for the Development and Production of Electronic Products,* New York City, NY: Institute for Electrical and Electronic Engineers (IEEE), 2012.

[4] *Failure Mechanism Based Stress Test Qualification for Integrated Circuits (AEC-Q100 Rev. H),* Automotive Electronics Council, 2014.

[5] *Stress-Test Driven Qualification of Integrated Circuits (JESD47K),* Joint Electron Device Engineering Council (JEDEC), 2018.

[6] *Failure Mechanism Based Stress Test Qualification for Discrete Semiconductors in Automotive Applications (AEC-Q101 Rev. E),* Automotive Electronics Council, 2021.

[7] *Reliability Qualification of Semiconductor Devices Based on Physics of Failure Risk and Opportunity Assessment (JEP148B),* Joint Electron Device Engineering Council (JEDEC), 2014.

[8] *Failure Mechanism Based Stress Test Qualification for Optoelectronic Semiconductors in Automotive Applications (AEC-Q102 Rev. A),* Automotive Electronics Council (AEC), 2020.

[9] C. Grosskopf, F. Xue, D. Locker, S. Thomas, J. Zheng and M. Tsuriya, "Benchmarking of Qualification Methodologies for New Package Technologies and Materials," in *International Conference on Electronics Packaging (ICEP)*, Niigata, Japan, 2019.

[10] *Application Specific Qualification Using Knowledge Based Test Methodology [JESD94B, Test Methodology Standard],* Arlington, VA, USA: Joint Electron Device Engineering Council (JEDEC), 2021 [Reaffirmed].

[11] *Stress-Test-Driven Qualification of and Failure Mechanisms Associated with Assembled Solid State SurfaceMount Components [Publication],* Arlington, VA, USA: Joint Electron Device Engineering Council (JEDEC), 2011 [Reaffirmed].

[12] *Department of Defense MIL-STD 883L: Test Method Standard Microcircuits,* Arlington, VA: U.S. Department of Defense, 2019.

[13] *Department of Defense MIL-STD 750E: Test Methods for Semiconductor Devices,* Arlington, VA: Department of Defense, USA, 2006.

[14] C. Grosskopf, F. Xue, D. Locker, S. Thomas, K. Zheng and M. Tsuriya, "iNEMI New Package/Material Qualification Methodology: Project Summary Report," International Electronics Manufacturing Initiative, 2020.

[15] *Department of Defense MIL-STD-810: Environmental Engineering Considerations,* Department of Defense, 2019.

[16] K. C. Kapur and M. Pecht, Reliability Engineering, A. P. Sage, Ed., Hoboken, NJ, USA: John Wiley & Sons, Inc., 2014.

[17] A. Ramakrishnan and M. Pecht, "Load Characterization During Transportation," *Microelectronics Reliability,* vol. 44, pp. 333-338, 2004.

[18] R. Valentin, J. Cunningham, C. Hillman, A. Dasgupta and M. Osterman, "A Demonstration of Virtual Qualification for the Design of Electronic Hardware," in *Institute of Environmental Sciences and Technology (IEST),* Phoenix, AZ, USA, 2001.

[19] S. Peyghami, H. Wang, P. Davari and F. Blaabjerg, "Mission-Profile-Based System-Level Reliability Analysis in DC Microgrids," *IEEE Transactions on Industry Applications,* vol. 55, no. 5, pp. 5055-5067, 2019.

[20] K. Ma, S. Xia, Y. Qi, X. Cai, Y. Song and F. Blaabjerg, "Power-Electronics-Based Mission Profile Emulation and Test for Electric Machine Drive System - Concepts, Features, and Challenges," *IEEE Transactions on Power Electronics*, vol. 37, no. 7, pp. 8526 - 8542, 2022.

[21] J. Karppinen, *Reliability Assessment of Electronic Assemblies Under Multiple Interacting Loading Conditions [Doctoral Dissertation]*, Espoo, Finland: School of Electrical Engineering, Aalto University, 2013.

[22] K. D. Cluff, D. Robbins, T. Edwards and D. B. Barker, "Characterizing the Commercial Avionics Thermal Environment for Field Reliability Assessment," *Journal of the Institute of Environmental Sciences*, vol. 40, no. 4, pp. 22-28, 1997.

[23] FIDES Guide 2009: Reliability Methodology for Electronic Systems, A ed., FIDES, 2012.

[24] R. Valentin, J. Cunningham, M. Osterman, A. Dasgupta, M. G. Pecht and D. Tsagos, "Virtual Life Assessment of Electronic Hardware Used in the Advanced Amphibious Assault Vehicle," in *Winter Simulation Conference*, San Diego, CA, USA, 2002.

[25] *J-STD-020: Moisture/Reflow Sensitivity Classification for Nonhermetic Surface Devices*, Arlington, VA: Joint Electron Device Engineering Council (JEDEC), 2014.

[26] B. Song, *Impact of Dust on the Reliability of Printed Circuit Assemblies*, College Park, Maryland: University of Maryland, College Park, 2012.

[27] M. Matsuishi and T. Endo, "Fatigue of Metals Subjected to Varying Stress," in *Japan Society of Mechanical Engineers*, Fukuoka, Japan, 1968.

[28] Y.-L. Lee and T. Tjhung, "Rainflow Cycle Counting Techniques," in *Metal Fatigue Analysis Handbook*, Butterworth-Heinemann, 2012, pp. 89-114.

[29] *Standard Practices for Cycle Counting in Fatigue Analysis (ASTM E1049-85),* West Conshohocken, PA: American Society for Testing and Materials, 2011.

[30] D. Ribeiro, R. Calçada and R. Delgado, "Fatigue of Metallic Railway Bridges: Implementation of a Methodology of Analysis and Application to the Alcácer do Sal Bridge," in *The Third International Conference on Bridge Maintenance, Safety and Management*, Porto, Portugal, 2006.

[31] C. D. Souto, J. A. Correia, A. M. De Jesus and R. A. Calçada, "Fatigue Damage Tool (FDT) - A Tool for Fatigue Damage Assessment According to Design Codes," *Procedia Structural Integrity,* vol. 22, pp. 376-385, 2019.

[32] C. Pace, J. Hernandez-Ambato, L. Fragomeni, G. Consentino, A. D'Ignoti, S. Galiano and A. Grimaldi, "A New Effective Methodology for Semiconductor Power

Devices HTRB Testing," *IEEE Transactions on Industrial Electronics,* vol. 64, no. 6, pp. 4857 - 4865, 2016.

[33] L. Yang and A. Castellazi, "High Temperature Gate-Bias and Reverse-Bias Tests on SiC MOSFETs," *Microelectronics Reliability,* vol. 53, pp. 1771 - 1773, 2013.

[34] Y. Cheng, G. Fu, M. Jiang and P. Xue, "Investigation on Intermittent Life Testing Program for IGBT," *Journal of Power Electronics,* vol. 17, no. 3, pp. 811 - 820, 2017.

[35] Y. Chen and B. Hou, "Intermittent Operating Life Results for Different Control Strategies," in *16th International Conference on Electronic Packaging Technology (ICEPT)*, Changsha, China, 2015.

[36] F. Hoffmann and N. Kaminski, "Investigation on the Impact of Environmental Stress on the Thermo-Mechanical Reliability of IGBTs by Means of Consecutive H3TRB and PCT Testing," in *33rd International Symposium on Power Semiconductor Devices and ICs (ISPSD)*, [Virtual Conference], 2021.

[37] P. S. Chauhan, "PHM-Based Qualification of Electronics," in *Prognostics and Health Management of Electronics: Fundamentals, Machine Learning, and the Internet of Things*, M. G. Pecht and M. Kang, Eds., IEEE Press, Wiley, 2018, pp. 329 - 248.

[38] C. Zorn and N. Kaminski, "Acceleration of Temperature Humidity Bias (THB) Testing on IGBT Modules by High Bias Levels," in *27th International Symposium on Power Semiconductor Devices & IC's*, Hong Kong, 2015.

[39] Z. Ni, X. Lyu, O. P. Yadav and D. Cao, "Review of SiC MOSFET Based Three-Phase Inverter Lifetime Prediction," in *IEEE Applied Power Electronics Conference and Exposition (APEC)*, Tampa, FL, USA, 2017.

[40] F. C. Classe and S. Gaddamraja, "Long Term Isothermal Reliability of Copper Wire Bonded to Thin 6.5 µm Aluminum," in *International Reliability Physics Symposium*, Monterey, CA, USA, 2011.

[41] L. A. Escobar and W. Q. Meeker, "A Review of Accelerated Test Models," *Statistical Science*, vol. 21, no. 4, pp. 552-577, 2006.

[42] K. C. Boyko and D. L. Gerlach, "Time Dependent Dielectric Breakdown of 210 Å Oxides," in *27th Annual Proceedings., International Reliability Physics Symposium*, Phoenix, AZ, USA, 1989.

[43] *Integrated Circuits (Microcircuits) Manufacturing, General Specification For [MIL-PRF-38535J]*, Columbus, OH: United States Department of Defense, 2010.

[44] S. Stoyanov, G. Tourloukis and C. Bailey, "Similarity Based Reliability Qualification of Electronic Components," in *38th International Spring Seminar on Electronics Technology (ISSE)*, Eger, Hungary, 2015.

[45] W. D. van Driel, G. Q. Zhang and L. J. Ernst, "Structural Similarity as a Method to Reduce Qualification Tests," in *6th International Conference on Electronic Packaging Technology*, Shenzhen, China, 2005.

[46] S. Stoyanov, C. Bailey and G. Tourloukis, "Similarity Approach for Reducing Qualification Tests of Electronic Components," *Microelectronics Reliability,* vol. 67, pp. 111-119, 2016.

[47] S. Stoyanov, M. Ahsan, C. Bailey, T. Wotherspoon and C. Hunt, "Predictive Analytics Methodology for Smart Qualification Testing of Electronic Components," *Journal of Intelligent Manufacturing,* vol. 30, pp. 1497-1514, 2019.

[48] M. Pecht, T. Shibutani, M. Kang, M. Hodkiewicz and E. Cripps, "A fusion prognostics-based qualification test methodology for microelectronic products," *Microelectronics Reliability,* vol. 63, pp. 320-324, 2016.

[49] M. Pecht and J. Gu, "Prognostics-Based Product Qualification," *IEEEAC,* 2009.

[50] G. Zhang, D. Das, R. Xu and M. Pecht, "IDDQ Trending as a Precursor to Semiconductor Failure," in *International Conference on Prognostics and Health Management*, Denver, Colorado, USA, 2008.

[51] N. Patil, D. Das, K. Goebel and M. Pecht, "Identification of Failure Precursor Parameters for Insulated Gate Bipolar Transistors (IGBTs)," in *International Conference on Prognostics and Health Management*, Denver, CO, USA, 2008.

[52] W. Kexin, D. Mingxing, X. Linlin and L. Jian, "Study of Bonding Wire Failure Effects on External Measurable Signals of IGBT Module," *IEEE Transactions on Device and Materials Reliability,* vol. 14, no. 1, pp. 83-89, 2014.

[53] N. Patil, J. Celaya, D. Das, K. Goebel and M. Pecht, "Precursor Parameter Identification for Insulated Gate Bipolar Transistor (IGBT) Prognostics," *IEEE Transactions on Reliability,* vol. 58, no. 2, pp. 271-276, 2009.

[54] V. Smet, F. Forest, J.-J. Huselstein, F. Richardeau, Z. Khatir, S. Lefebvre and M. Berkani, "Ageing and Failure Modes of IGBT Modules in High in High Temperature Power Cycling," *IEEE Transactions on Industrial Electronics,* vol. 58, no. 10, pp. 4931-4941, 2011.

[55] B. Ji, V. Pickert, W. Cao and B. Zahawi, "In Situ Diagnostics and Prognostics of Wire Bonding Faults in IGBT Modules for Electric Vehicle Drives," *IEEE Transactions on Power Electronics,* vol. 28, no. 12, pp. 5568-5577, 2013.

[56] S. Dusmez, S. H. Ali, M. Heydarzadeh, A. S. Kamath, H. Duran and B. Akin, "Aging Precursor Identification and Lifetime Estimation for Thermally Aged Discrete Package Silicon Power Switches," *IEEE Transactions on Industry Applications,* vol. 53, no. 1, pp. 251-260, 2017.

[57] A. Oukaour, B. Tala-Ighil, B. Pouderoux, M. Tounsi, M. Bouarroudj-Berkani, S. Lefebvre and B. Boudart, "Ageing Defect Detection on IGBT Power Modules by Artificial Training Methods Based on Pattern Recognition," *Microelectronics Reliability,* vol. 51, pp. 386-391, 2011.

[58] H. Zhang, R. Kang, M. Luo and M. Pecht, "Precursor Parameter Identification for Power Supply Prognostics and Health Management," in *8th International Conference on Reliability, Maintainability and Safety*, Chengdu, China, 2009.

[59] A. E. Ginart, D. W. Brown, P. W. Kalgren and M. J. Roemer, "Online Ringing Characterization as a Diagnostic Technique for IGBTs in Power Drives," *IEEE Transactions on Instrumentation and Measurement,* vol. 58, no. 7, pp. 2290-2299, 2009.

[60] S. Zhou, L. Zhou and P. Sun, "Monitoring Potential Defects in an IGBT Module Based on Dynamic Changes of the Gate Current," *IEEE Transactions on Power Electronics*, vol. 28, no. 3, pp. 1479-1487, 2012.

[61] T. A. Nguyen, S. Lefebvre, P.-Y. Joubert, D. Labrousse and S. Bontemps, "Estimating Current Distributions in Power Semiconductor Dies Under Aging Conditions: Bond Wire Liftoff and Aluminum Reconstruction," *IEEE Transactions on Components, Packaging, and Manufacturing Technology,* vol. 5, no. 4, pp. 483-495, 2015.

[62] J. Liu, G. Zhang, Q. Chen, L. Qi, Y. Geng and J. Wang, "In situ Condition Monitoring of IGBTs Based on the Miller Plateau Duration," *IEEE Transactions on Power Electronics,* vol. 34, no. 1, pp. 769-782, 2019.

[63] B. Ji, X. Song, W. Cao, V. Pickert, Y. Hu, J. W. Mackersie and G. Pierce, "In Situ Diagnostics and Prognostics of Solder Fatigue in IGBT Modules for Electric Vehicle Drives," *IEEE Transactions on Power Electronics,* vol. 30, no. 3, pp. 1535-1543, 2015.

[64] N. Baker, M. Liserre, L. Dupont and Y. Avenas, "Improved Reliability of Power Modules: A Review of Online Junction Temperature Measurement Methods," *IEEE Industrial Electronics Magazine,* vol. 8, no. 3, pp. 17-27, 2014.

[65] H. Kuhn and A. Mertens, "On-Line Junction Temperature Measurement of IGBTs Based on Temperature Sensitive Electrical Parameters," in *13th European Conference on Power Electronics and Applications*, Barcelona, Spain, 2009.

[66] M. Ciappa, "Selected Failure Mechanisms of Modern Power Modules," *Microelectronics Reliability,* vol. 45, no. 4-5, pp. 653-667, 2002.

[67] C. Wang, Y. He, C. Wang, L. Li and X. Wu, "Multi-Chip IGBT Module Failure Monitoring Based on Module Transconductance with Temperature Calibration," *Electronics,* vol. 9, no. 10, pp. 1-17, 2020.

[68] E. Sutrisno*, Fault Detection and Prognostics of Insulated Gate Bipolar Transistor (IGBT) Using a K-Nearest Neighbor Classification Algorithm [Thesis],* College Park, MD: University of Maryland, 2013.

[69] G. Guo, H. Wang, D. Bell, Y. Bi and K. Greer, "KNN Model-Based Approach in Classification," in *On the Move to Meaningful Internet Systems 2003: CoopIS, DOA, and ODBASE,* Catania, Sicily, Italy, OTM Confederated International Conferences, 2003, pp. 986 - 996.

[70] N. Patil, D. Das and M. Pecht, "Anomaly detection for IGBTs using Mahalanobis distance," *Microelectronics Reliability,* vol. 55, pp. 1054-1059, 2015.

[71] N. Patil, D. Das and M. Pecht, "Mahalanobis Distance Approach to Field Stop IGBT Diagnostics," in *Proceedings of the 10th International Seminar on Power Semiconductors*, Prague, Czech Republic, 2010.

[72] N. Patil, S. Menon, D. Das and M. Pecht, "Anomaly Detection of Non Punch Through Insulated Gate Bipolar Transistors (IGBT) by Robust Covariance Estimation Techniques," in *2nd International Conference on Reliability, Safety and Hazard - Risk-Based Technologies and Physics-of-Failure Methods (ICRESH)*, Mumbai, India, 2010.

[73] N. Patil, S. Menon, D. Das and M. Pecht, "Evaluation of Robust Covariance Estimation Techniques for Anomaly Detection of Insulated Gate Bipolar Transistors (IGBT)," in *ASME 2010 Conference on Smart Materials, Adaptive Structures and Intelligent Systems*, Philadelphia, Pennsylvania, USA, 2010.

[74] X. Liu, L. Liu, D. Das, I. H. Naqvi and M. Pecht, "Online Degradation State Assessment Methodology for Multi-mode Failures of Insulated Gate Bipolar Transistor," *IEEE Access*, vol. 8, pp. 69471 - 69481, 2020.

[75] Y. Lu and A. Christou, "Prognostics of IGBT Modules Based on the Approach of Particle Filtering," *Microelectronics Reliability*, vol. 92, pp. 96-105, 2019.

[76] T. Tinga and R. Loendersloot, "Physical Model-Based Prognostics and Health Monitoring to Enable Predictive Maintenance," in *Predictive Maintenance in Dynamic Systems*, E. Lughofer and M. Sayed-Mouchaweh, Eds., Springer, 2019, pp. 313-352.

[77] N. Patil, D. Das and M. Pecht, "A Prognostic Approach for Non-Punch Through and Field Stop IGBTs," *Microelectronics Reliability*, vol. 52, pp. 482-488, 2011.

[78] K. Hu, Z. Liu, H. Du, L. Ceccarelli, F. Blaabjerg and I. A. Tasiu, "Cost-Effective Prognostics of IGBT Bond Wires with Consideration of Temperature Swing," *IEEE Transactions on Power Electronics (Regular Paper/Letter/Correspondence)*, vol. 35, no. 7, pp. 6773-6784, 2019.

[79] P. Thodi, F. Khan and M. Haddara, "Risk Based Integrity Modeling of Gas Processing Facilities Using Bayesian Analysis," in *Proceedings of the 1st Annual Gas Processing Symposium*, Doha, Qatar, 2009.

[80] J. Elfring, E. Torta and R. van de Molengraft, "Particle Filters: A Hands-On Tutorial," *Sensors*, vol. 21, no. 438, pp. 1-28, 2021.

[81] T. Sreenuch, A. Alghassi, S. Perinpanayagam and Y. Xie, "Probabilistic Monte-Carlo Method for Modelling and Prediction of Electronics Component Life," in *(IJACSA) International Journal of Advanced Computer Science and Applications*, 2014.

[82] S. H. Ali, M. Heydarzadeh, S. Dusmez, X. Li, A. S. Kamath and B. Akin, "Lifetime Estimation of Discrete IGBT Devices Based on Gaussian Process," *IEEE Transactions on Industry Applications,* vol. 54, no. 1, pp. 395-403, 2018.

[83] A. Alghassi, S. Perinpanayagam and M. Samie, "Stochastic RUL Calculation Enhanced With TDNN [Time Delay Neural Network]-Based IGBT Failure Modeling," *IEEE Transactions on Reliability,* vol. 65, no. 2, pp. 558-573, 2015.

[84] T. Wang, J. Yu, D. Siegel and J. Lee, "A Similarity-Based Prognostics Approach for Remaining Useful Life Estimation of Engineered Systems," in *International Conference on Prognostics and Health Management*, Denver, CO, USA, 2008.

[85] D. F. Maio and E. Zio, "Failure Prognostics by a Data-Driven Similarity-Based Approach," *International Journal of Reliability, Quality and Safety Engineering,* vol. 20, no. 1, pp. 1-17, 2013.

[86] "IKD06N60R," Infineon Technologies, 2014.

[87] T. Laska, M. Münzer, F. Pfirsch, C. Schaeffer and T. Schmidt, *The Field Stop IGBT (FS IGBT) - A New Power Device Concept with a Great Improvement Potential,* Toulouse, France: Proceedings of the 2nd International Symposium on Power Semiconductor Devices and ICs, 2000.

[88] F. P. Vandrevala, *Modeling and Characterization of the Insulated Gate Bipolar Transistor in the Near-Threshold Region [Master's Thesis]*, Arlington, Texas, USA: University of Texas at Arlington, 2013.

[89] M. Harada, T. Minato, H. Takahashi, H. Nishihara, K. Inoue and I. Takata, "600V Trench IGBT in Comparison with Planar IGBT: An Evaluation of the Limit of IGBT Performance," in *Proceedings of the 6th International Symposium on Power Semiconductor Devices and Ics*, Davos, Switzerland, 1994.

[90] V. K. Khanna, Insulated Gate Bipolar Transistor IGBT Theory and Design, Piscataway, New Jersey, USA: Institute of Electrical and Electronics Engineers (IEEE), 2003.

[91] M. H. Rashid, Power Electronics Handbook: Devices, Circuits and Applications, Burlington, Massachusetts, USA: Butterworth-Heinemann, 2011.

[92] H. Yilmaz, J. L. Benjamin, R. F. Dyer, Jr., L.-S. S. Chen, W. R. Van Dell and G. C. Pifer, "Comparison of the Punch-Through and Non-Punch-Through IGT Structures," *IEEE Transactions on Industry Applications*, vol. 1A, no. 22, pp. 466-470, 1986.

[93] *Fuji IGBT Modules Application Manual*, Tokyo, Japan: Fuji Electric Co.,Ltd., 2015.

[94] M. Osterman, "CALCE Simulation Assisted Reliability Assessment (SARA) Software," University of Maryland, College Park, Maryland, USA, 2020.

[95] N. Patil, D. Das, K. Goebel and M. Pecht, "Failure Precursors for Insulated Gate Bipolar Transistors," in *9th International Seminar on Power Semiconductors*, Prague, Czech Republic, 2008.

[96] N. Valentine, *Failure Modes and Mechanisms Analysis of Silicon Power Devices*, College Park, MD, USA: University of Maryland, College Park, 2017.

[97] S. H. Ali, E. Ugur and B. Akin, "Analysis of Vth Variations in IGBTs Under Thermal Stress for Improved Condition Monitoring in Automotive Power Conversion Systems," *IEEE Transactions on Vehicular Technology,* vol. 68, no. 1, pp. 193-202, 2019.

[98] H. Meng, Y. Wang, X. Zheng, J. Chen, Y. Wu, A. Li and Y. Huang, "Study of IGBTs Reliability Under Coupled Electrical-Thermal Environment," *IEEE Journal of Emerging and Selected Topics in Power Electronics,* vol. 9, no. 4, pp. 4260-4268, 2020.

[99] B. Wang, Y. Tang and M. Chen, "Experimental Study on Voltage Breakdown Characteristic of IGBT," in *Asia-Pacific Power and Energy Engineering Conference*, Wuhan, China, 2011.

[100] Jacquemont, C.; Wong, K. M.; Goh, David, "Hydrogen Proton Induced HTRB Reliability Degradation in Trench Power Devices," in *IEEE Electron Devices Technology and Manufacturing Conference Proceedings of Technical Papers*, Penang, Malaysia, 2020.

[101] D. Goh, W. J. Chen, F. Tahir, S. P. Lee and V. C. Ngwan, "HTRB & THB Reliability Improvement Using Capping Layer in Power Discrete Trench Devices," in *5th IEEE Electron Devices Technology & Manufacturing Conference (EDTM),* Chengdu, China, 2021.

[102] L. E. Nelson, "The Shewhart Control Chart—Tests for Special Causes," *Journal of Quality Technology,* vol. 16, no. 4, pp. 237-239, 1984.

[103] P. C. Mahalanobis, "On the Generalized Distance in Statistics," *Proceedings of the National Institute of Sciences of India,* vol. 2, no. 1, pp. 49-55, 1936.

[104] "Particle Filter Workflow [Online Website]," MathWorks, Natick, Massachusetts, USA, 1994-2022.